Institutionen för systemteknik
Department of Electrical Engineering

Examensarbete

Massive MIMO in LTE with MRT Precoder: Channel Ageing and Throughput Analysis in a Single-Cell Deployment

Examensarbete utfört i Kommunikationssystem
vid Tekniska högskolan vid Linköpings universitet
av

Henrik Rydén

LiTH-ISY-EX--14/4762--SE

Linköping 2014

Department of Electrical Engineering
Linköpings universitet
SE-581 83 Linköping, Sweden

Linköpings tekniska högskola
Linköpings universitet
581 83 Linköping

Massive MIMO in LTE with MRT Precoder: Channel Ageing and Throughput Analysis in a Single-Cell Deployment

Examensarbete utfört i Kommunikationssystem
vid Tekniska högskolan vid Linköpings universitet
av

Henrik Rydén

LiTH-ISY-EX--14/4762--SE

Handledare: **Christopher Mollén**
ISY, Linköpings universitet
Reza Moosavi
Ericsson AB

Examinator: **Danyo Danev**
ISY, Linköpings universitet

Linköping, 13 juni 2014

Avdelning, Institution
Division, Department

Kommunikationssystem
Department of Electrical Engineering
SE-581 83 Linköping

Datum
Date

2014-06-13

Språk
Language

☐ Svenska/Swedish
☒ Engelska/English
☐ _____

Rapporttyp
Report category

☐ Licentiatavhandling
☒ Examensarbete
☐ C-uppsats
☐ D-uppsats
☐ Övrig rapport
☐ _____

ISBN
—

ISRN
LiTH-ISY-EX--14/4762--SE

Serietitel och serienummer
Title of series, numbering

ISSN
—

URL för elektronisk version
http://urn.kb.se/resolve?urn=urn:nbn:se:liu:diva-XXXXX

Titel
Title

Massiv MIMO i LTE med MRT förkodning: kanalåldring och datataktanalyser i ett system med en basstation

Massive MIMO in LTE with MRT Precoder: Channel Ageing and Throughput Analysis in a Single-Cell Deployment

Författare
Author

Henrik Rydén

Sammanfattning
Abstract

Mobile data traffic is growing exponentially due to the popularization of smart phones, tablets and other data traffic appliances. One way of handling the increased data traffic is to deploy large antenna arrays at the base station, also known as Massive MIMO. In Massive MIMO, the base station having excessive number of transmit antennas, can achieve increased data rate by spatial-multiplexing terminals into the same time-frequency resource.

This thesis investigates Massive MIMO in LTE in a single-cell deployment with up to 100 base station antennas. The benefits of more antennas are investigated with single-antenna terminals in a typical urban environment. The terminal transmitted sounding reference signals (SRS) are used at the base station to calculate channel state information (CSI) in order to generate an MRT precoder. With perfect CSI, the results showed that the expected terminal SINR depends on the antenna-terminal ratio. It was also showed that with spatial-multiplexed terminals and 100 base station antennas, the maximum cell throughput increased 13 times compared with no spatial-multiplexed terminals.

Channel ageing causes inaccuracy in the CSI, the thesis showed that the variation in terminal SINR increased rapidly with less frequent SRS transmissions. When having moving terminals at 3 km/h, the difference between the 10th and 90th SINR percentile is 1 dB with an SRS transmission periodicity of 20 ms, and 17 dB with an SRS transmission periodicity of 80 ms. With 100 base station antennas and moving terminals at 3 km/h with an SRS periodicity of 20 ms, the maximum cell throughput decreased with 13% compared to when the base station has perfect CSI.

The result showed that the maximum cell throughput scaled linearly with the number of base station antennas. It also showed that having the number of spatial-multiplexed terminals equal to the number of antennas is a reasonable assumption when maximizing the cell throughput.

Nyckelord
Keywords

Massive MIMO, Channel Ageing, LTE, MRT

Abstract

Mobile data traffic is growing exponentially due to the popularization of smart phones, tablets and other data traffic appliances. One way of handling the increased data traffic is to deploy large antenna arrays at the base station, also known as Massive MIMO. In Massive MIMO, the base station having excessive number of transmit antennas, can achieve increased data rate by spatial-multiplexing terminals into the same time-frequency resource.

This thesis investigates Massive MIMO in LTE in a single-cell deployment with up to 100 base station antennas. The benefits of more antennas are investigated with single-antenna terminals in a typical urban environment. The terminal transmitted sounding reference signals (SRS) are used at the base station to calculate channel state information (CSI) in order to generate an MRT precoder. With perfect CSI, the results showed that the expected terminal SINR depends on the antenna-terminal ratio. It was also showed that with spatial-multiplexed terminals and 100 base station antennas, the maximum cell throughput increased 13 times compared with no spatial-multiplexed terminals.

Channel ageing causes inaccuracy in the CSI, the thesis showed that the variation in terminal SINR increased rapidly with less frequent SRS transmissions. When having moving terminals at 3 km/h, the difference between the 10th and 90th SINR percentile is 1 dB with an SRS transmission periodicity of 20 ms, and 17 dB with an SRS transmission periodicity of 80 ms. With 100 base station antennas and moving terminals at 3 km/h with an SRS periodicity of 20 ms, the maximum cell throughput decreased with 13% compared to when the base station has perfect CSI.

The result showed that the maximum cell throughput scaled linearly with the number of base station antennas. It also showed that having the number of spatial-multiplexed terminals equal to the number of antennas is a reasonable assumption when maximizing the cell throughput.

Acknowledgments

This work was performed at Ericsson Research in Linköping Sweden during the spring of 2014.

I would like to thank my supervisors at Ericsson, Reza Moosavi and Erik Eriksson. They have thoroughly explained the problems I have encountered despite their full schedules and have shown great interest in my work. I would like to express my gratitude to LINLAB for the superb atmosphere and the exciting table hockey matches.

I would also like to thank Christopher Mollén at Linköping University for improving the quality of the report by carefully reading it multiple times. Thank you for guiding me with the structure of the report and making me realize that writing takes more time than I first expected.

Linköping, June 2014
Henrik Rydén

Contents

Notation

Notation	Meaning
M	Number of base station antennas
K	Number of terminals
α	$\frac{M}{K}$
β_k	Real valued, large-scale fading coefficient for terminal k
$\gamma_{k,m}$	Complex number, small-scale fading coefficient for terminal k to antenna m
$h_{k,m}$	Complex number, the channel from terminal k to antenna m
$\boldsymbol{h_k}$	Complex vector, the channel vector from terminal k to antenna array
$\boldsymbol{q}$	Symbol vector
$\boldsymbol{w_k}$	Precoding weights for the symbol intended for terminal k
$\|\cdot\|$	The 2-norm, $\|\boldsymbol{x}\| = (\sum_{m=1}^{\dim(\boldsymbol{x})} \|x_m\|^2)^{1/2}$
$[\cdot]^*$	Complex-conjugate transpose of a matrix or a vector

Abbrevations

Abbrevation	Meaning
ACF	Autocorrelation Function
ARQ	Automatic Repeat Request
BS	Base Station
CDF	Cumulative-Distribution Function
CRC	Cyclic Redundancy Check
CRS	Cell-Specific Reference Signal
CSI	Channel-State Information
EPDCCH	Enhanced Physical-Downlink Control-Channel
FDD	Frequency-Division-Duplex
ITU	International Telecommunication Union
LTE	Long-Term Evolution
MCS	Modulation and Coding-Scheme
MIMO	Multiple-Input Multiple-Output
MRT	Maximum-Ratio Transmission
OFDM	Orthogonal Frequency-Division Multiplexing
PDCCH	Physical-Downlink Control-Channel
PDSCH	Physical-Downlink Shared-Channel
PUCCH	Physical-Uplink Control-Channel
PUSCH	Physical-Uplink Shared-Channel
QAM	Quadrature Amplitude Modulation
QPSK	Quadrature-Phase Shift-Keying
SINR	Signal-to-Interference-plus-Noise Ratio
SIR	Signal-to-Interference Ratio
SRS	Sounding Reference Signal
TDD	Time-Division-Duplex

1 Introduction

This chapter will give an introduction to the work in this thesis together with the problem formulation.

1.1 Background

Mobile data traffic is growing exponentially due to the enormous success of smart phones, tablets and other data traffic appliances. One way of handling the increased wireless data traffic is to deploy more base stations (BS) and densify the cellular network. This would however increase interference and deployment cost. Another less explored option for increasing the data rate is to introduce large antenna arrays at the BS, which is seemingly simpler in terms of deployment cost. By introducing hundreds of antennas at the BS, performance gains can be achieved in comparison to the LTE standard that supports up to 8 antenna ports at the BS. The downside is new problems for the industry and academia to tackle such as designing the physical antenna array.

In systems with Massive MIMO (also known as "Very Large MIMO "), the BS can achieve increased data rate by scheduling multiple terminals at the same time, and into the same frequency band, this is also referred to as the same *time-frequency resource*. The gains are achieved without buying any additional spectrum.

1.2 Problem Formulation

When introducing significantly more antennas, beamforming and spatial multiplexing techniques can be utilized. This thesis investigates Massive MIMO in LTE and evaluates the gains of multiple BS antennas by using an LTE simulator. The

thesis will only consider downlink transmission in a single cell and will make use of the terminal transmitted uplink pilot symbols to acquire channel state information (CSI). The channel is assumed to be reciprocal and the channel estimates are used to generate a maximum ratio transmission (MRT) precoder [12].

This thesis will investigate

1. How do spatial-multiplexing terminals into the same time-frequency resource affect the expected SINR and the throughput?
2. How does channel ageing affect SINR?
3. How does the chosen LTE configuration in Chapter 4 affect the CSI acquisition and the maximum terminal throughput?
4. What is the ratio between the number of BS antennas and the number of terminals that maximizes the cell throughput?
5. What is the required number of BS antennas in order to maximize the terminal throughput?

1.3 Thesis Overview

Chapter 1 gives an introduction to the problem.
Chapter 2 gives the relevant Massive MIMO theory for this thesis.
Chapter 3 explains the relevant parts of LTE for this thesis.
Chapter 4 outlines the simulator setup and discusses the thesis assumptions.
Chapter 5 presents the results.
Chapter 6 discusses how the chosen LTE configuration affect the CSI acquisition and the maximum terminal throughput.
Chapter 7 answers the questions from the problem statement.
Chapter 8 suggests some of the further research needed.

2

Massive MIMO Theory

This chapter describes the Massive MIMO theory regarding a single cell with M BS antennas and K single-antenna terminals.

2.1 Overview

In Massive MIMO, the BS has a large amount of antennas. There is no definition of how many antennas is large, this study will investigate up to 100 BS antennas. Massive MIMO relies on spatial-multiplexing the K terminals into the same time-frequency resource which requires the BS to have good enough channel knowledge. The channel knowledge for downlink is obtained for an LTE system by transmitting pilot symbols that let the terminal estimate the channel responses. The resources needed for downlink pilot symbols scales with the number of antennas and will thus grow large in a Massive MIMO system with hundreds of antennas. The general solution is to let the terminals transmit pilot symbols and through reciprocity, assume that the downlink and uplink channel are the same [11].

By shaping the signals transmitted from each BS antenna, the wave fronts emitted by each antenna can be made to add constructively at the intended terminals and destructively to the other terminals. Figure 2.1 shows the idea with Massive MIMO systems, where multiple BS antennas send independent data streams to multiple terminals in the same time-frequency resource.

The effects of adding more antennas are more diversity and the effects of additive receiver noise and small-scale fading disappear when the number of antennas grows large due to the law of large numbers, as shown by [15].

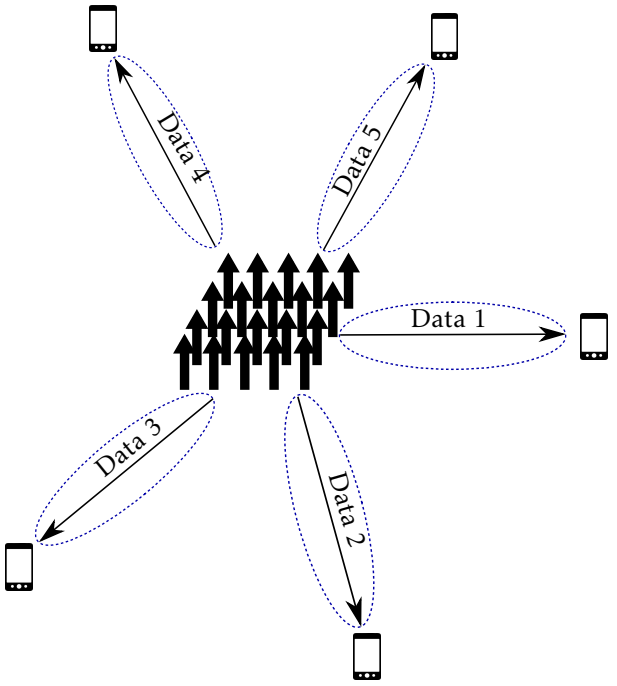

Figure 2.1: *BS with multiple antennas sends independent data streams to multiple terminals in the same time-frequency resource.*

Massive MIMO requires the BS to have accurate channel knowledge and imposes challenges when the channel changes rapidly. The number of simultaneously served terminals is limited by the inability to acquire channel knowledge for an unlimited amount of terminals and not by the number of antennas [17]. The time allocated for acquiring channel knowledge dictates the number of served terminals but with the trade-off for the time spent sending data to the terminals, the trade-off is showed analytically in [14].

2.2 Signal Model

The BS is interested in sending a $K \times 1$ symbol vector $\boldsymbol{q}$ to K terminals. The channels from the M antennas to the K terminals are modelled as a $K \times M$ complex valued matrix H which is referred to as the *Channel Matrix*,

$$H = \begin{bmatrix} h_{1,1} & h_{1,2} & \cdots & h_{1,M} \\ h_{2,1} & h_{2,2} & \cdots & h_{2,M} \\ \vdots & \vdots & \ddots & \vdots \\ h_{K,1} & h_{K,2} & \cdots & h_{K,M} \end{bmatrix}.$$

Figure 2.2 illustrates the elements in the channel matrix. The exact model for the

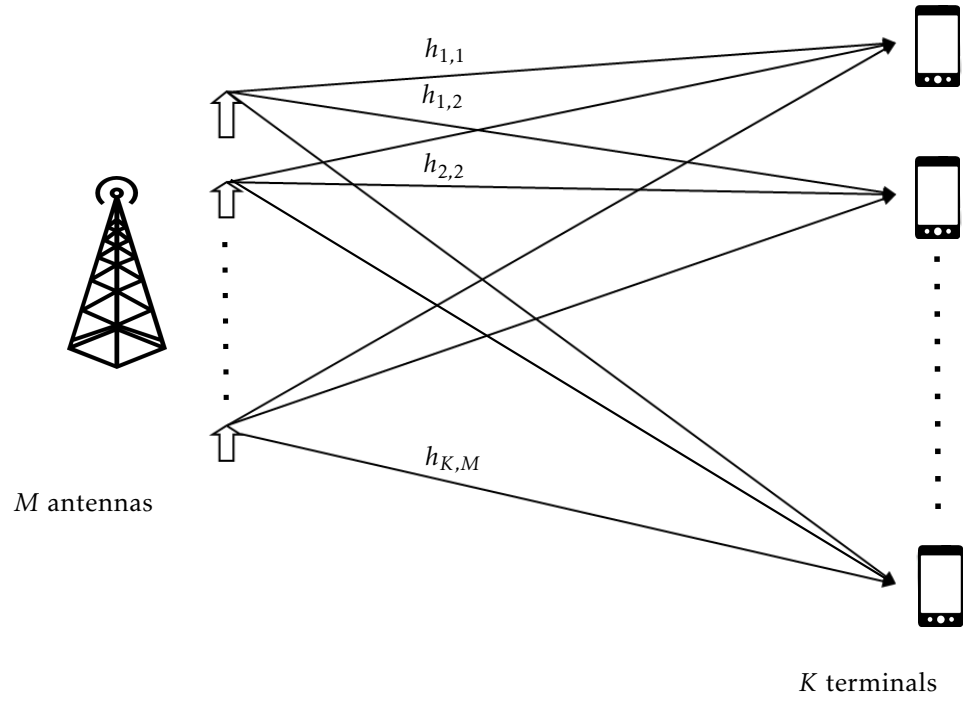

Figure 2.2: *Channel model for Massive MIMO.*

channel matrix will be made clear in the subsequent discussions.

The K terminals receive their respective component in the $K \times 1$ vector $\boldsymbol{y}$,

$$\boldsymbol{y} = H\boldsymbol{x} + \boldsymbol{e}, \tag{2.1}$$

where $\boldsymbol{x}$ is the precoded symbol vector $\boldsymbol{q}$ and $\boldsymbol{e}$ is additive white Gaussian noise with i.i.d. components $e_k \sim \mathcal{CN}(0, N_0)$.
The energy constraint of the i-th element in $\mathbf{q}$ is

$$\mathbb{E}\{q_i^* q_i\} = 1, \quad i = 1, \ldots, K. \tag{2.2}$$

The BS uses CSI in order to precode the symbols. Let W be a complex valued $M \times K$ precoding matrix with $\|W\| = 1$, let p be the BS transmission power. The transmit vector $\boldsymbol{x}$ is generated by

$$\boldsymbol{x} = \sqrt{p} W \boldsymbol{q}. \tag{2.3}$$

The transmitted symbol on the i-th antenna can be written as

$$x_i = \sqrt{p} \sum_{j=1}^{K} w_{i,j} q_j. \tag{2.4}$$

The k-th terminal receives

$$y_k = \sqrt{p} \sum_{m=1}^{M} h_{k,m} x_m + e_k = \sqrt{p} \sum_{j=1}^{K} \sum_{m=1}^{M} h_{k,m} w_{m,j} q_j + e_k. \tag{2.5}$$

By identifying the useful part when $j = k$, we can write the equation as

$$y_k = \sqrt{p} \sum_{m=1}^{M} h_{k,m} w_{m,k} q_k + \sqrt{p} \sum_{j \neq k} \sum_{m=1}^{M} h_{k,m} w_{m,j} q_j + e_k, \tag{2.6}$$

where the useful term is the first term. The Signal-to-Interference-plus-Noise Ratio (SINR) for terminal k is

$$\text{SINR} = \frac{\mathbb{E}\left(\left| \sqrt{p} \sum_{m=1}^{M} h_{k,m} w_{m,k} q_k \right|^2 \right)}{\mathbb{E}\left(\left| \sqrt{p} \sum_{j \neq k} \sum_{m=1}^{M} h_{k,m} w_{m,j} q_j \right|^2 \right) + \mathbb{E}\left(|e_k|^2 \right)}. \tag{2.7}$$

The precoder studied in this project is the MRT precoder. According to the MRT precoding, the transmitted signal from each antenna is formed in such a way that the received signal from each antenna adds up coherently at the terminal which maximizes the received power. This is often referred as the *beamforming*. The *beamforming gain* is the power gain that is achieved by using multiple antennas compared to using a single antenna.

Assuming perfect CSI, the transmitted symbol vector $\boldsymbol{q}$ are precoded with the MRT precoder according to

$$W = \frac{H^*}{\|H\|}, \tag{2.8}$$

where H^* is the complex conjugate transpose of the channel matrix. $\|H\|$ is the 2-norm of the channel matrix. The k-th column in W is the precoding vector for terminal k and can be written as

$$\boldsymbol{w}_k = \frac{\boldsymbol{h}_k^*}{\|H\|}. \tag{2.9}$$

2.3 Limitations of Massive MIMO

This section describes the limitations of Massive MIMO that will be investigated in this thesis.

2.3.1 Interference with MRT Precoding

When scheduling multiple terminals in the same time-frequency resource, they interfere with each other. According to [17], for i.i.d. circularly symmetric Gaussian channels with mean zero and variance 1, the expected terminal SINR with

perfect transmit CSI, when using the MRT precoder is

$$\text{SINR} = \frac{\rho\alpha}{\rho+1}, \alpha \triangleq \frac{M}{K} \text{ when } M, K \to \infty, \tag{2.10}$$

where ρ is the average transmitted power divided by the noise variance. This result states that the SINR is limited by α when ρ is large. The interference in this thesis is studied by changing M and K.

2.3.2 Delayed CSI Error

The BS calculates CSI for each terminal from the uplink pilot symbols. In this thesis, the channel is reciprocal and the BS has perfect CSI at time of uplink pilot transmission. The inaccuracy of the CSI is affected by *channel ageing*, the variations in channel strength over time. The channel varies between when it is learned at the BS and when it is used for beamforming. There is an error factor if the channel coherence time is less than the delay between receiving CSI and the downlink transmission. The error from using old CSI in downlink transmission is also known as the *delayed CSI error*.

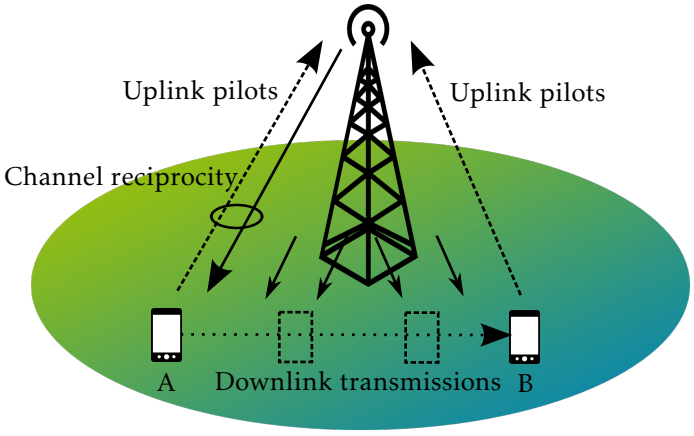

Figure 2.3: *Moving terminal from point A to point B. The channel estimates from point A will be used at the BS for precoding downlink transmissions until the next channel estimate from uplink pilot transmission at point B.*

The delayed CSI error in this thesis is studied by changing the terminal velocity and the uplink pilot transmission periodicity. Figure 2.3 illustrates the problem with the delayed CSI error for a moving terminal. The intuition is that the delayed CSI error will be largest when the terminal is close to point B. In this thesis, the distance between point A and B is in order of centimeters. Additionally, the channel is assumed to be constant for non-moving terminals, they will therefore not suffer from the delayed CSI error. The BS will then have perfect CSI at all downlink transmissions to the non-moving terminals.

2.4 Performance

The expected sum rate can be upper bounded by using Shannons theoretical boundary and (4.3),

$$C_{sum} \leq K \log_2(1 + \mathbb{E}(\text{SINR})) = K \log_2(1 + \frac{\rho M/K}{\rho + 1}). \tag{2.11}$$

This equation is valid for $K < M$, and the sum rate is plotted in Figure 2.4 for different number of antennas with $\rho = 13$ dB.

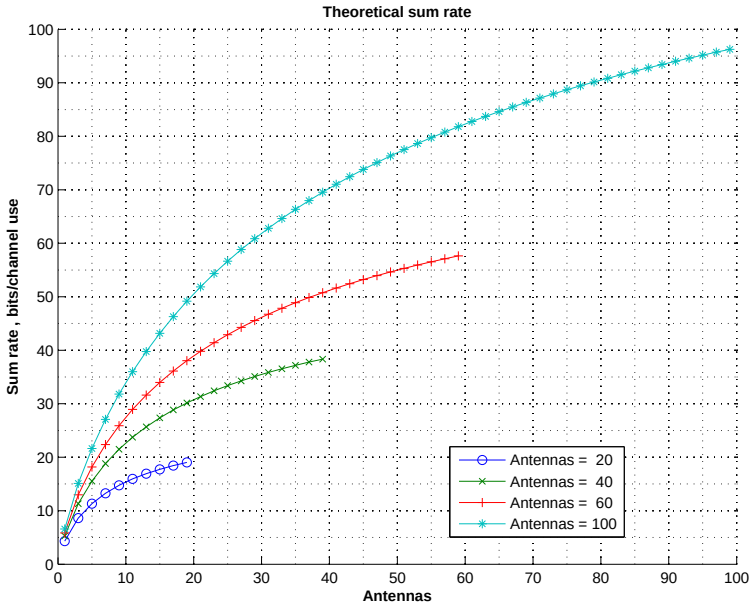

Figure 2.4: *Sum rate from* (2.11)

2.5 Channel Model

In wireless systems, *fading* is time variation in channel strength caused by small-scale effect of multipath and larger-scale effects such as geometric attenuation and shadowing by obstacles.

Small-scale fading is due to the propagation environment causes multiple versions of the transmitted signal to arrive at the receiver. This occurs at the spatial scale of the order of the carrier wavelength and is frequency dependent. *Large-scale fading* is due to path loss of the signal as a function of the distance to the BS and by shadowing from buildings or the landscape [20].

The complex channel in this thesis is modelled as

$$h_{k,m} = \beta_k \gamma_{k,m} \tag{2.12}$$

$$k = 1, \ldots, K$$

$$m = 1, \ldots, M$$

where $\gamma_{k,m}$ is referred to as the small-scale fading coefficient and β_k as the large-scale fading coefficient. For terminal k, the antennas have the same large-scale fading coefficient while the small-scale coefficients $\gamma_{k,m}$ are i.i.d. circularly symmetric Gaussian with mean zero and variance 1. The correlation in time and frequency for each $\gamma_{k,m}$ is given by the International Telecommunication Union (ITU) typical urban model, see [1].

3

LTE Overview

This chapter gives an overview of LTE and describes more in detail the parts of LTE that concerns this thesis.

3.1 Orthogonal Frequency-Division Multiplexing

Orthogonal Frequency-Division Multiplexing (OFDM) is the transmission scheme used in LTE and is a kind of multi-carrier transmission. The symbol $B[n]$ is modulated onto its own subcarrier $e^{j2\pi n\Delta f t}$, where the subcarrier spacing $\Delta f = 1/T$, T is the symbol duration time. The discrete OFDM signal is given by

$$z[k] = \sum_{n=0}^{N-1} B[n] e^{j2\pi nk/N}, \quad k \geq 0 \tag{3.1}$$

where N is the number of OFDM subcarriers and during each OFDM symbol interval, N symbols are transmitted in parallel.

For LTE, the subcarrier spacing equals 15 kHz and the number of subcarriers depends on the bandwidth used by the system. The bandwidths for LTE release 8 is 1.4, 3, 5, 10, 15 and 20 MHz. The time-frequency grid for LTE is shown in Figure 3.1, where a column corresponds to an OFDM symbol. The smallest entity is called a *resource element* consisting of a single subcarrier in one OFDM symbol, a *resource block* is a block of 12 consecutive subcarriers during a 0.5 ms interval. Each resource block contains 84 resource elements. Resource blocks are defined over one slot and two consecutive slots creates a *subframe*. The minimum scheduling unit consists of two consecutive resource blocks within a subframe and is referred to as a *resource-block pair*. A *radioframe* consists of 10 subframes and the radioframe duration is 10 ms.

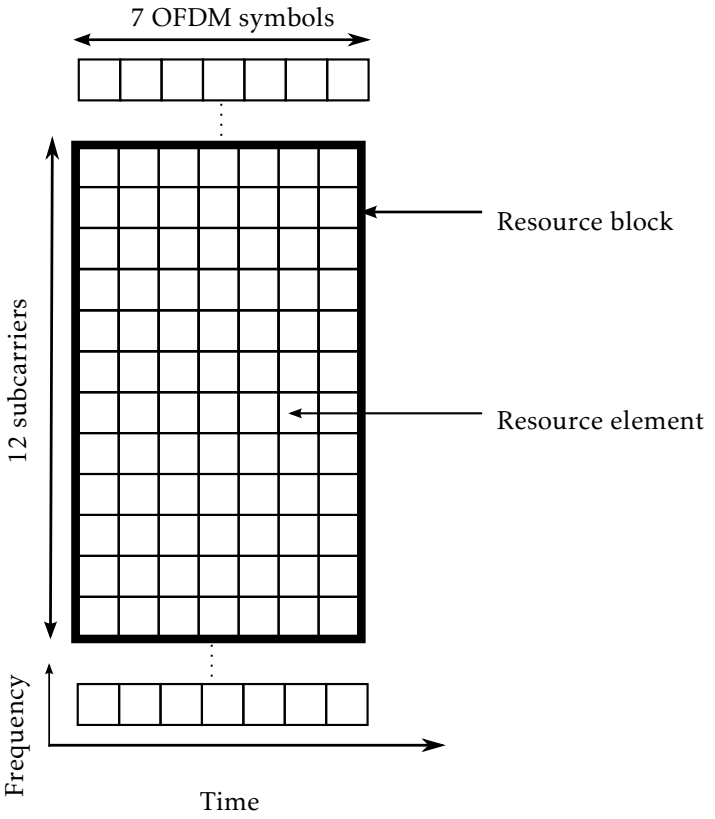

Figure 3.1: *Time-frequency grid for LTE.*

There are 140 OFDM symbols in a radioframe and when multiplying the number of OFDM symbols by the symbol duration T, we get a radioframe duration of 9.33 ms. The actual time of 10 ms is because of inserting a *cyclic prefix* for each OFDM symbol. The cyclic prefix insertion implies that the last L samples in the OFDM symbol is copied and inserted at the beginning of the symbol, that is, before we send the samples $z[0], \ldots, z[N-1]$, we transmit

$$z[k] = z[N+k], \quad k = -L, -(L-1), \ldots, -1.$$

The cyclic prefix increases the OFDM symbol duration by the cyclic prefix duration T_{CP}. The cyclic prefix is inserted to retain orthogonality for delayed versions of the received signal [7].

The time frame is illustrated in Figure 3.2.

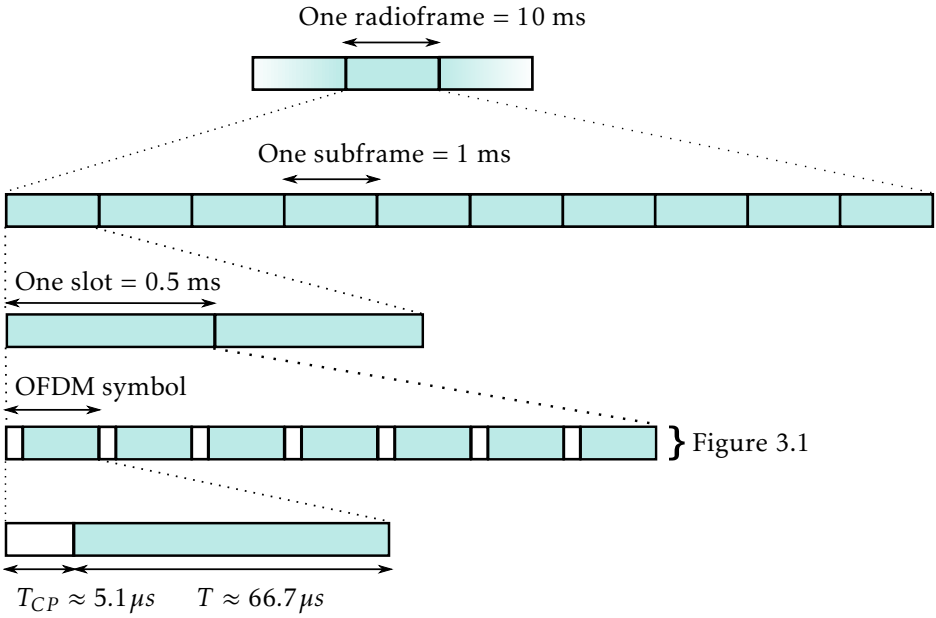

Figure 3.2: *Radioframe structure.*

3.2 Duplexing

The time-frequency resource allocation between uplink and downlink can be divided using two different strategies. The strategies are time-division-duplex (TDD) which separates the transmissions in time, and frequency-division-duplex (FDD) that separates the transmissions in frequency. In FDD, uplink and downlink transmissions can occur simultaneously when the terminals support full-duplex. Half-duplex is when downlink and uplink transmission need to be separated in time and the terminals need a guard interval to switch between reception and transmission.

The guard interval for TDD in LTE is handled by a *special subframe* which contains a downlink part (DwPTS), a guard period (GP) and an uplink part (UpPTS). The downlink part is used for regular downlink transmission but with the limitation of fewer resources compared to a normal downlink subframe. The guard period is used to let the BS and the terminals circuits to switch from downlink-uplink transmission and to ensure that downlink-uplink transmissions do not interfere. The UpPTS could be left empty and provide extra guard period or used for additional uplink pilot symbol transmissions.

The allocated resources for uplink and downlink in TDD are provided by seven different downlink/uplink configurations. The thesis assumes TDD and the next chapter will motivate the choice of downlink/uplink configuration.

3.3 Reference Signals

For a conventional LTE system, to properly demodulate the transmitted symbol $B[n]$, the terminal should have information about the channel. As shown by [7, section 3.5], the terminal multiplies the received signal with the conjugate of the frequency-domain channel tap. Pre-determined cell-specific reference signals (CRS) are sent from the BS at regular time-frequency intervals to allow the terminal to estimate the channel around the reference symbol in the time-frequency grid. The number of occupied resource elements for CRS transmissions are proportional to the number of antenna ports.

For uplink, the BS calculates channel estimations from the terminal transmitted *sounding reference signals* (SRS). The SRS transmission can be *periodic* where the SRS are transmitted at fixed periodicity and *aperiodic*, where the control channel triggers one-time SRS transmissions. The channel estimations for uplink can also be used to get downlink channel estimates for a TDD system, this property is the basis for this thesis implementation of Massive MIMO in an LTE system.

The CRS is not used in this thesis since the precoding is done via uplink channel estimation. Note that for coherent demodulation and effective channel estimation, downlink reference signals might be needed in Massive MIMO but are terminal specific compared to CRS which is unicast [16].[1] The resources for Massive MIMO downlink pilots are proportional to the number of terminals and not to the number of antennas. The downlink pilot symbols for Massive MIMO are not taken into account in this study.

3.4 Physical Channels

The time-frequency grid is divided in different physical channels, the relevant physical channels for this thesis are described briefly below.

PDCCH

Physical Downlink Control Channel (PDCCH) is used for downlink control signalling such as scheduling decisions for the Physical-Downlink Shared-Channel (PDSCH).

PDSCH

PDSCH is the main physical channel for downlink data transmission, PDCCH schedules the terminals so each terminal gets its own resource allocation in the PDSCH. For our Massive MIMO system, there will be multiple terminals in the same PDSCH resources.

[1] This terminal specific pilots is called demodulation reference signals (DM-RS) in LTE context [7].

3.5 Hybrid Automatic Repeat Request

Automatic Repeat Request is used to handle transmission errors, *Cyclic Redundancy Check* (CRC) is inserted to allow the receiver to detect transmission errors. The appended CRC bits is used by the receiver to check if the CRC bits agree with the data and the receiver transmits a *negative acknowledgement* (NACK), if an error has occurred. The transmitter then retransmits the information until a *positive acknowledgement* (ACK) is reported by the receiver. In this thesis, the transmission feedback is used for link adaptation which will be described in the next chapter.

The hybrid ARQ combines forward error correction and ARQ meaning that the ARQ reports when the received data contains uncorrectable errors. The basic idea in forward error correction is to introduce redundancy in the code to allow the receiver to correct a limited number of bits. LTE uses CRC for error detection and turbo code for error correction on the PDSCH. Turbo codes use convolution codes as building blocks to construct random-looking codes that perform close to Shannon-theoretic limits [13]. The idea of the turbo code is to create a randomization that creates dependencies between coded bits that are separated far away in time and thus, the diversity increases since the different parts of the codeword experience independent fades.

3.6 Downlink Transmission

The data bits for transmission is divided into *transport blocks*, one transport block of dynamic size can be sent during each transmission time interval of 1 ms corresponding to a single subframe.

The channel coding for PDSCH is based on a turbo coder. Before the channel coding, the transport block is segmented into separate *code blocks* to match the code-block sizes supported by the turbo coder [4]. The encoding consists of two rate-1/2 encoders with 3 memory elements, see Figure 3.3. The outputs from the two rate-1/2 rate encoders are transmitted along with the systematic bits from the first encoder which implies an overall code rate of 1/3. The output from the turbo coder is input to the rate matching and hybrid-ARQ functionality which extracts the set of coded bits that should be transmitted. The bit selection block selects the number of bits for transmission depending on the desired code rate. High number of bits gives a low code rate and vice versa. After the bit selection, the block of bits is multiplied bitwise by a scrambling sequence with the purpose to make the sequence of bits more random-like and to minimize the interference with neighbouring cells.

The scrambled bits are modulated using QPSK, 16QAM or 64QAM [3]. The use of QPSK gives 2 bits per symbol during a modulation-symbol interval while 16QAM gives 4 bits and 64QAM gives 6 bits. Use of higher modulation order provides higher data rate with the cost of reduced robustness to noise and interference.

LTE supports 29 different modulation and coding schemes (MCS) that will de-

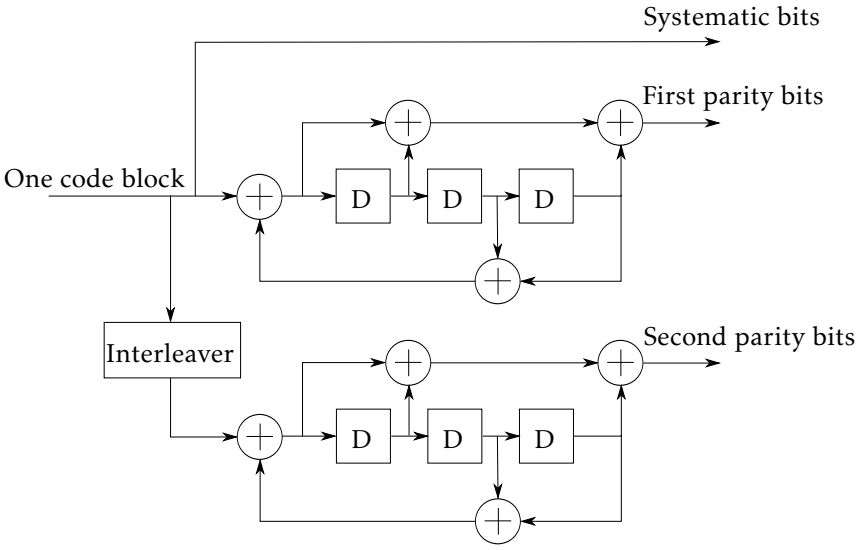

Figure 3.3: *Turbo encoder used in LTE.*

termine the data rate of the system. Higher MCS implies that larger transport blocks are transmitted. The modulation and coding rate depends on the channel conditions, some MCS might perform better under a certain condition which makes it important to adapt to the current channel condition. The choice of transmission parameters depending on the channel conditions is referred to as the link adaptation, the link adaptation for this thesis will be presented in the next chapter.

4

Simulator Setup

This chapter describes the simulator setup and the thesis assumptions.

4.1 Assumptions

The simulations are performed with an LTE simulator in TDD mode with the parameters according to [2, Table A.2.1.1-3]. Table 4.1 shows the important simulator parameters and assumptions, the assumptions will be explained more in detail in this chapter.

Bandwidth - 5 MHz
42% of the resource elements are allocated for downlink transmission
Cellular layout, 1 cell, 1 sector
Cell radius - 166 m
Central subcarrier - 2.00 GHz
Channel Model - ITU Typical Urban
TDD configuration 1
TDD special subframe configuration 8
BS transmitter power - 20 W
MRT precoder
Uncorrelated antennas
Terminals in full buffer mode
Reciprocal channel
Channel is constant for non-moving terminals

Table 4.1: *Simulator setup*

The simulations are performed in Ericssons internal simulator.

4.2 Acquiring CSI

The channel estimations are based on the SRS in uplink. Based on reciprocity, the channel estimations in uplink are used to generate a linear precoder in the downlink. The terminals are configured to have periodic SRS transmissions.

There are limited amount of resources for SRS transmissions which implies that the terminals need to share this limited amount of resources. A longer SRS transmission periodicity for each terminal increases the maximum number of served terminals due to each terminal uses less SRS resources, the downside of less frequent SRS transmission is higher delayed CSI error since the BS precodes with old channel estimates for a longer time.

The SRS transmissions periodicity is a multiple of 5 ms for the thesis chosen TDD configuration, see Figure 4.1. In this thesis, the channel is assumed to be constant over one resource-block pair and during one OFDM symbol, 12 terminals can transmit SRS. The last OFDM symbol in uplink is reserved for SRS transmission, see Figure 4.2b, the number of uplink subframes combined with the SRS periodicity gives the limitation of the maximum number of served terminals in a cell. Table 4.2 shows how the maximum number of served terminals depends on the SRS transmission frequency for some SRS periodicities.

SRS periodicity [ms]	5	10	20	30	40	60	80
Maximum number of terminals	24	48	96	144	192	240	384

Table 4.2: *Maximum number of served terminals for different SRS periodicities.*

4.3 MRT Implementation

Since the BS calculates CSI individually for each terminal based on the arrival of the SRS, the simulator implementation of the precoder for terminal k is

$$\boldsymbol{w}_k = \frac{\boldsymbol{h}_k^*}{\sqrt{K}\|\boldsymbol{h}_k\|}. \tag{4.1}$$

Thus, compared with (2.9), the precoder in the simulator is not normalized with $\|H\|$. The signal-to-interference ratio (SIR) for terminal k is calculated by using (2.6), with w_k from (4.1). Using the channel model (2.12) and the fact that the large-scale fading coefficient and the small-scale coefficient are independent, the

SIR for terminal k is

$$\begin{aligned}
\text{SIR} &= \frac{\mathbb{E}\left(\left|\sqrt{p}q_k \frac{\boldsymbol{h_k}\boldsymbol{h_k}^*}{\sqrt{K}\|\boldsymbol{h_k}\|}\right|^2\right)}{\mathbb{E}\left(\left|\sqrt{p}\sum_{j\neq k} q_j \frac{\boldsymbol{h_k}\boldsymbol{h_j}^*}{\sqrt{K}\|\boldsymbol{h_j}\|}\right|^2\right)} = \frac{\mathbb{E}\left(\left|\frac{\beta_k^2(|\gamma_{k,1}|^2+\cdots+|\gamma_{k,m}|^2)}{\sqrt{\beta_k^2(|\gamma_{k,1}|^2+\cdots+|\gamma_{k,m}|^2)}}\right|^2\right)}{\mathbb{E}\left(\left|\sum_{j\neq k} q_j \frac{\beta_k\beta_j(\gamma_{k,1}\gamma_{j,1}^*+\cdots+\gamma_{k,m}\gamma_{j,m}^*)}{\sqrt{\beta_j^2(|\gamma_{j,1}|^2+\cdots+|\gamma_{j,m}|^2)}}\right|^2\right)} \\
&= \frac{\mathbb{E}(|\beta_k|^2)\mathbb{E}\left(\left|\frac{(|\gamma_{k,1}|^2+\cdots+|\gamma_{k,m}|^2)}{\sqrt{(|\gamma_{k,1}|^2+\cdots+|\gamma_{k,m}|^2)}}\right|^2\right)}{\mathbb{E}(|\beta_k|^2)\mathbb{E}\left(\left|\sum_{j\neq k} q_j \frac{\beta_j(\gamma_{k,1}\gamma_{j,1}^*+\cdots+\gamma_{k,m}\gamma_{j,m}^*)}{\sqrt{\beta_j^2(|\gamma_{j,1}|^2+\cdots+|\gamma_{j,m}|^2)}}\right|^2\right)} \\
&= \frac{\mathbb{E}\left(\left|\frac{(|\gamma_{k,1}|^2+\cdots+|\gamma_{k,m}|^2)}{\sqrt{(|\gamma_{k,1}|^2+\cdots+|\gamma_{k,m}|^2)}}\right|^2\right)}{\mathbb{E}\left(\left|\sum_{j\neq k} q_j \frac{(\gamma_{k,1}\gamma_{j,1}^*+\cdots+\gamma_{k,m}\gamma_{j,m}^*)}{\sqrt{(|\gamma_{j,1}|^2+\cdots+|\gamma_{j,m}|^2)}}\right|^2\right)} = \frac{\mathbb{E}\left(|\gamma_{k,1}|^2+\cdots+|\gamma_{k,m}|^2\right)}{\mathbb{E}\left(\left|\sum_{j\neq k} q_j \frac{(\gamma_{k,1}\gamma_{j,1}^*+\cdots+\gamma_{k,m}\gamma_{j,m}^*)}{\sqrt{(|\gamma_{j,1}|^2+\cdots+|\gamma_{j,m}|^2)}}\right|^2\right)}. \qquad (4.2)
\end{aligned}$$

The equation states that the SIR for the terminals is independent of the large-scale fading coefficient. In this thesis, we operate in an interference limited regime, i.e., the noise power is very small compared to the transmitted power and therefore, the performance is limited mainly by the interference. We will therefore assume that the SINR is approximately the SIR when spatial-multiplexing terminals into the same time-frequency resource, i.e., when $K > 1$.

The author of this thesis was not able to show that (4.2) scales linearly as α when M and K is large. The thesis will even though use α as the theoretical boundary and as the simulations will show, it is a reasonable assumption.

The expected terminal SINR is therefore

$$\text{SINR} = \alpha. \qquad (4.3)$$

4.4 TDD Setup

The simulator uses TDD configuration 1 and the structure is shown in figure 4.1. The motivation for the chosen TDD configuration is to have more downlink subframes than uplink subframes since data traffic statistics show that the downlink traffic load is larger than the uplink traffic load [6]. The figure illustrates the special subframe and its three components. The special subframe was set arbitrarily to configuration 8, where DwPTS uses 11 OFDM symbols and GP + UpPTS uses 3 OFDM symbols. The choice of special subframe will affect the number of resources assigned for downlink transmission, however, this thesis is interested in increasing the cell throughput with multiple BS antennas, and not how to increase the throughput by using another resource allocation.

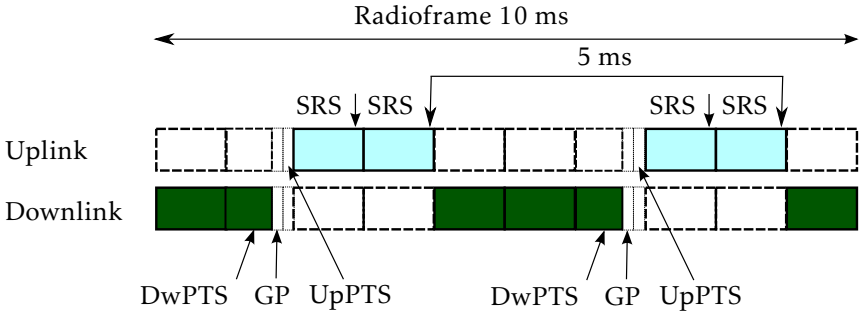

Figure 4.1: *TDD configuration and the location for the SRS.*

Since the bandwidth is 5 MHz, each subframe contain 25 resource-block pairs [7]. The layout of the resource-block pair for a normal downlink subframe is shown in figure 4.2a. The special subframe has the same structure as the normal subframe but the last three OFDM symbols are reserved for GP and UpPTS.

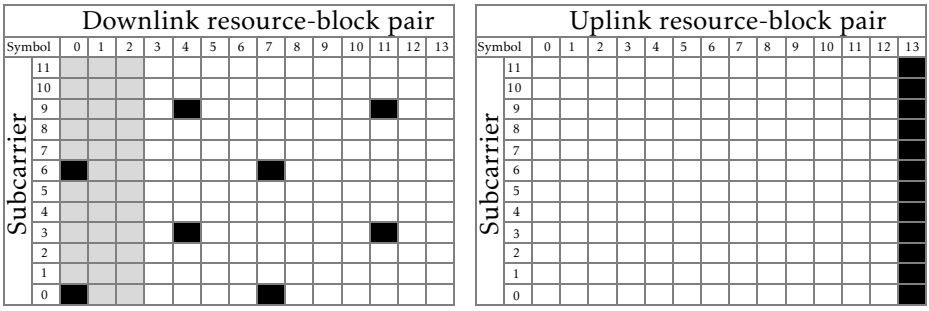

(a) *Black = CRS, Grey = PDCCH, White = PDSCH*

(b) *Black = SRS, White = physical uplink channels*

Figure 4.2: *Structure of a normal downlink resource-block pair and the structure of an uplink resource-block pair.*

The choice of TDD configuration will affect the result in this thesis. If prioritizing more uplink subframes, there are more resources for SRS and therefore, we could serve more terminals. The cost of more uplink subframes is of course less downlink subframes and the downlink throughput decreases.

LTE contains broadcast channels in some subframes but these are disregarded for simplicity, this implies a slight optimistic result in terms of throughput since we use the resources allocated for broadcast channels for the PDSCH.

4.5 Scheduling

The scheduling limitations is not taken into account, the PDCCH has a limited amount of resources and can not schedule an unlimited amount of terminals. The simulator is configured to let all the terminals with pending data reception to be scheduled in all PDSCH resources. There are 3 OFDM symbols allocated in each downlink subframe for the PDCCH channel in order to include resource allocation for control signalling to create a more realistic resource allocation.

4.6 Link Adaptation

Link adaptation takes the radio-link quality into account to set the MCS. Perfect link adaptation cannot be achieved due to the random nature of radio-link quality and noise at the receiver. The hybrid ARQ is used at the BS to receive requests for retransmissions when the terminal could not decode the transport block, i.e., when the terminal transmit a negative acknowledgement. The *block error rate* is the error rate of the transport block transmissions.

The simulator is using an algorithm that adapts the MCS depending on the acknowledgement in the hybrid ARQ reports, the target is a fixed block error rate of 10% meaning that 90% of the transport blocks are transmitted successfully. The effective MCS will then be adapted to the SINR in the 10th percentile.

4.7 Theoretical Throughput Boundaries

The number of PDSCH resource elements in a downlink subframe are calculated by removing the resource elements allocated for CRS, PDCCH, GP and UpPTS. The number of resource elements for PDSCH is 25×126 for a normal subframe and 25×104 for the special subframe. Modulation with 64QAM and code rate 1 gives 6 bits of information per resource element. The maximum number of transmitted information bits in a radioframe using 5 MHz bandwidth is $6 \times 25 \times (4 \times 126 + 2 \times 104) = 106800$. The radioframe duration of 10 ms gives a throughput of 10.68 Mbps which is the maximum terminal throughput since the highest modulation is used and the code rate is 1. This configuration with code rate 1 is not valid in LTE and the next chapter will simulate the maximum terminal throughput.

By dividing the number of PDSCH resource-elements with the total number of resource-elements in a radioframe, we get that 42% of the resource elements are allocated for downlink data transmission.

4.8 Antenna Correlation

The physical antenna placement affects the correlation between two different antenna pairs. A physical antenna spacing of one half subcarrier wavelength is

sufficient with beneficial scattering environment [20]. It is pointed out in [17] that the antennas need to be placed far enough from other antennas in order to avoid major coupling and antenna correlation. In practice, measurements by [9] showed that there is correlation in two arbitrary chosen channel vectors to some extent, but the correlation decreases when increasing the number of BS antennas. Antenna correlation is not in the scope of this thesis, the thesis will assume that the antennas are uncorrelated.

4.9 Deployment Models

The terminals are spread uniformly over the grey area in Figure 4.3. The randomness of the terminals position needs to be taken into consideration since the terminals position affect the large-scale fading coefficient. The terminal large-scale fading coefficient varies when the terminal is moving but the simulator is configured to have the large-scale fading coefficient set to the value from its initial position. Note that equation (4.2) showed that the effect of large-scale fading disappear with our MRT precoder when having interference from other terminals. The large-scale fading coefficient will be investigated by simulating terminals without interference.

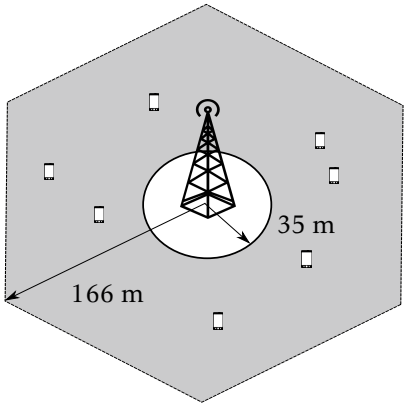

Figure 4.3: *Cell deployment with a cell radius of 166 meters and with uniformly distributed terminals over the grey area.*

4.10 Definitions

- *Throughput* - Terminal throughput is the data rate for each terminal and the cell throughput is the sum of the terminals throughput. For example, if 10 terminals each download a 1 Mbit file during an one second interval, the terminal throughput is 1 Mbps and the cell throughput is 10 Mbps. The thesis will only investigate downlink transmission and *throughput* implies downlink throughput.

- *Spatial-multiplexed terminals* - For simplicity, spatial-multiplexed terminals implies that the terminals are scheduled into the same time-frequency resource in downlink transmission.
- *No spatial-multiplexed terminals* - The terminals are scheduled into separate time resources.
- *Full Buffer* - Terminal continuously download at whatever data rate they can achieve [2]. This means that the terminal occupies all resource-elements in the PDSCH. The full buffer model assumes that the number of terminals in a cell remains constant.
- *Antenna-terminal ratio* - The ratio between the number of BS antennas and the number of served terminals, also defined as α.
- The SINR and throughput results will be presented by plotting the cumulative distribution function (CDF) in logarithmic scale. Let y represent the probability that the random variable X takes a value less than or equal to x such as

  $$y = \Pr(X < x) = \mathrm{CDF}(x).$$

  Consider SINR as our random variable X, we define the 10th SINR percentile for the x that satisfy

  $$0.1 = \mathrm{CDF}(x).$$

  The other SINR percentiles are defined likewise.

5
Simulation Results

This chapter presents the simulation results.

5.1 No Spatial-Multiplexed Terminals

The simulations in this section assume no spatial-multiplexed terminals and therefore, there is no interference from other terminals since we only consider a single-cell deployment. The large-scale fading will affect the result in this section since there is no interference. This section will simulate the terminal SINR for different number of BS antennas, since there is no interference, the figures will basically present the signal-to-noise ratio (SNR).

5.1.1 Single Terminal Simulations

The SINR for a single moving terminal at 3 km/h is simulated over 1, 4, 20, 40 and 100 BS antennas under the same channel conditions. Figure 5.1 shows how the SINR increases with the number of antennas and how the variation in SINR decreases with more antennas. The increased mean SINR for more antennas is because of the beamforming gain described in section 2.2, the less fluctuations in the channel is because of the channel hardening effect described in [20, section 8.2]. The noisy shape of the curves is because of the delayed CSI error which will be investigated in section 5.4.

Figure 5.2 shows a CDF over the SINR and it further concludes less variations in SINR when using more antennas. The figure shows that even with 4 antennas, the difference between the 1th and the 90th SINR percentile is 4 dB compared to 9 dB with a single-antenna. The difference for the 20, 40 and 100 antenna case is less than 2 dB in the same percentile interval. The gain in SINR is linear with the

number of antennas, doubling the number of antennas gives a 3 dB gain which is seen by comparing the 20 and 40 antenna curves.

The terminal SINR is affected by the transmitter power and the large-scale fading coefficient which is related to the terminal initial position. The simulation aimed to show the affects of multiple BS antennas under the same channel conditions and another initial position would give another large-scale fading coefficient and different result. Note that another initial terminal position would give the same characteristics in terms of beamforming gain and SINR variations, but would result in a movement of the curves along the SINR axis.

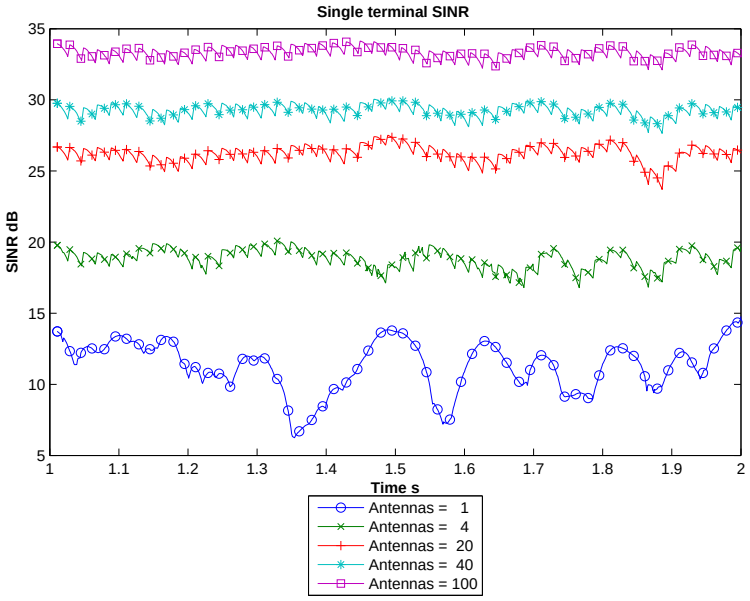

Figure 5.1: *SINR for a single terminal without interference.*

5.1.2 SINR to Terminal Throughput Relation

The terminal throughput depends on the SINR, a simulation is performed to investigate the maximum terminal throughput. The result is going to be utilized in later sections to calculate the required number of BS antennas in order to maximize the terminal throughput. The terminal from previous section is simulated with 100 BS antennas and the SINR is regulated by adjusting the BS transmitter power. The simulated terminal had SINR $\approx$ 35 dB with 100 BS antennas when transmitting at full power (20W).

The relation between the mean SINR and terminal throughput is illustrated in Figure 5.3. The figure shows that when the SINR is approximately 20 dB, the terminal throughput saturates at 9 Mbps, which means that the modulation is 64QAM and the code rate cannot be higher. The theoretical result of the maxi-

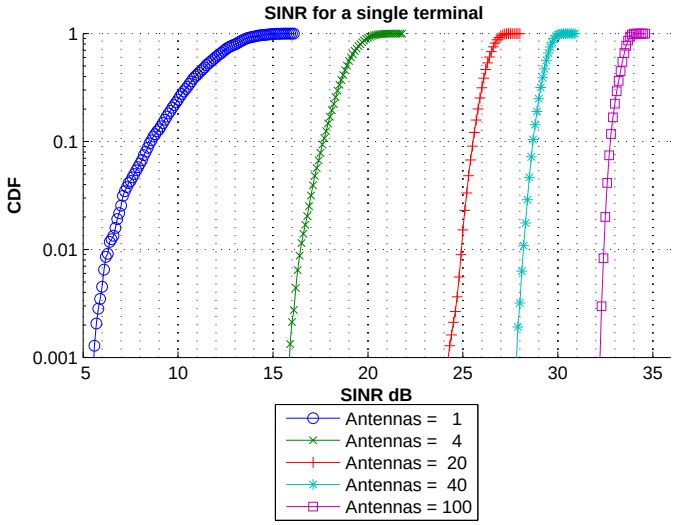

Figure 5.2: *SINR CDF for a single terminal without interference.*

mum throughput in section 4.7 gave a maximum cell throughput of 10.68 Mbps, while in the simulation, the maximum throughput is approximately 9 Mbps. The deviation from the theoretical value is due to the fact that the transport block sizes only take values according to [5, Table 7.1.7.2.1] and the simulator has a limitation on the maximum code rate. Note that 9 Mbps is also the maximum throughput of the cell with no spatial-multiplexed terminals since the terminal is in full buffer mode and uses all downlink transmission resources. We will in subsequent sections show how the cell throughput increases with spatial-multiplexed terminals.

The figure shows that the throughput is constant when the SINR is above 20 dB. This means that a BS with 100 antennas can reduce the transmitting power up to 14 dB under the current terminal propagation channel without any loss in throughput. If the standard had supported higher modulations such as 128QAM, we could instead make use of the beneficial SINR to increase the terminal throughput.

5.1.3 Large-Scale Fading

The large-scale fading coefficient depends as mentioned before on the geometric attenuation and shadowing. We will therefore investigate the SINR for multiple terminals without interference. The result is used in next section to examine (4.2), that the effect of large-scale fading diminishes with spatial-multiplexed terminals.

The simulated terminals are spatial-multiplexed into separate time resources and will therefore not have any interference from other terminals. The CDF of the

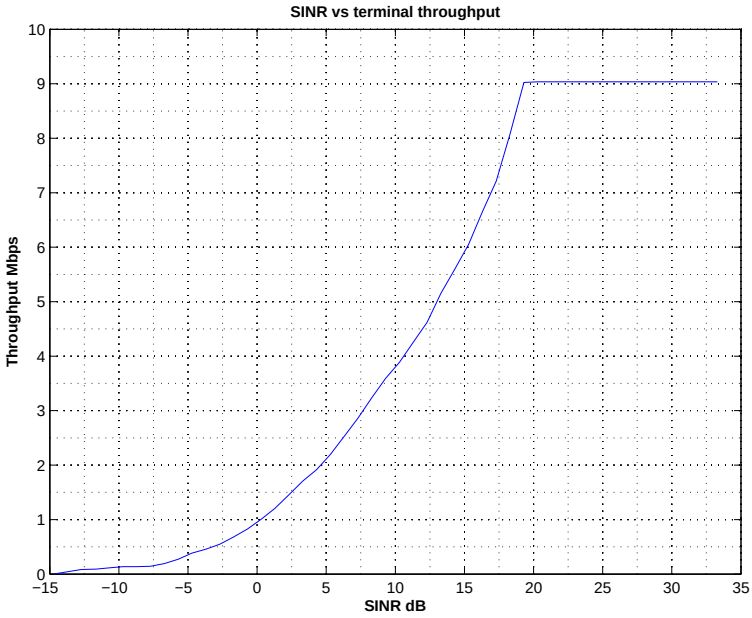

Figure 5.3: *Terminal throughput for different SINR.*

SINR is displayed in Figure 5.4. The figure shows that the terminal simulated in Figure 5.1 had a very bad SINR compared to the other terminals. The SINR for the mentioned terminal had SINR $\approx$ 35 dB with 100 BS antennas, which means that 97% of the terminals have a better SINR than the mentioned terminal. If we look at the 10th SINR percentile with 100 BS antennas, the SINR is 45 dB, by utilizing the result that the throughput saturates at SINR $\approx$ 20 dB, we could state that the BS can reduce its transmission power with 25 dB without any loss of performance for 90% of the terminals.

The rest of the Chapter will assume spatial-multiplexed terminals.

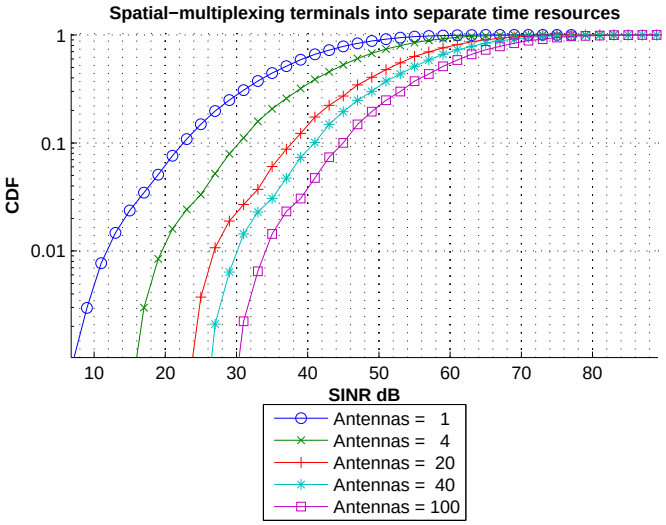

Figure 5.4: *SINR distribution when spatial-multiplexing terminals into separate time resources.*

5.2 SINR with Spatial-Multiplexed Terminals

The SINR with spatial-multiplexed terminals is studied by adjusting the number of terminals and the number of antennas. The simulations are performed with non-moving terminals and do not include the delayed CSI error from section 2.3.2.

Figure 5.5 shows the SINR with 40 BS antennas when adjusting the number of spatial-multiplexed terminals. We observe how the SINR decreases due to more interference when increasing the number of spatial-multiplexed terminals. With the MRT precoder that we applied in this thesis, i.e. (4.1), the effect of large-scale fading diminishes when having interference from other terminals, see (4.2). That is, all terminals experience more or less similar SINR. That is the reason why we for example see that the difference between the 10th and 90th SINR percentile when simulating 40 terminals is less than 2 dB. Comparing the results in Figure 5.5 with those in Figure 5.4, with no spatial-multiplexed terminals, there is no interference from other terminals and the large-scale fading coefficient is significant. We observe in Figure 5.4, there is approximately 35 dB difference between the 10th and the 90th SINR percentile for the case with 40 BS antennas. We can conclude that the effect of large-scale fading diminishes with spatial-multiplexed terminals by observing how the variations in SINR, with 40 BS antennas, decreases in Figure 5.5 compared to Figure 5.4. In other words, the terminal SINR is not affected by the distance to the BS when having interference from other terminals.

The theoretical SINR in (4.3) states that the expected SINR is limited by the

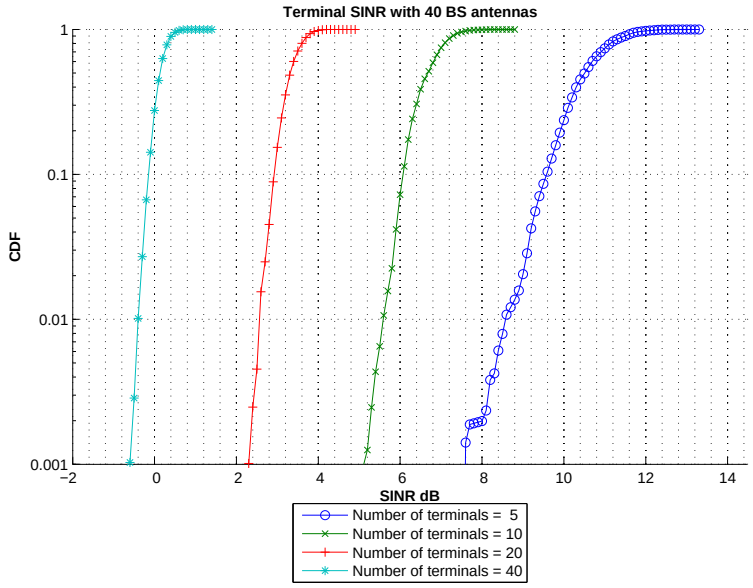

Figure 5.5: *SINR for non-moving terminals and with 40 BS antennas.*

antenna-terminal ratio. Note that increasing the transmitter power does not reduce the interference since increasing power creates more interference power as well. Equation (4.3) gives that doubling the number of spatial-multiplexed terminals would result in a 3 dB loss in SINR. The 3 dB loss in SINR can be seen in Figure 5.5 when for example the number of spatial-multiplexed terminals is increased from 5 to 10, or 10 to 20.

Figure 5.6 shows the SINR with 100 BS antennas with the same set of terminals from the 40 BS antennas case. We can also in this figure observe the 3 dB loss in SINR when doubling the number of terminals. The mean SINR for 10 terminals is approximately 10.5 dB, the mean SINR for 20 terminals is approximately 7.5 dB. When increasing the number of BS antennas with a factor of 2.5, the result should be approximately a 4 dB increase in SINR. This can also be seen in the figures since the curves are shifted by 4 dB when comparing the 40 BS antennas and the 100 BS antennas figures.

The asymptotic SINR in (4.3) is compared to the mean of the simulated SINR values in Figure 5.7. The figure shows that the simulated SINR values are slightly higher than the theoretical values, they are less than 1 dB separated when the number of terminals is more than 10. As seen in the figure, the simulated SINR converges to the asymptotic curve when the number of terminals increases. We can conclude that (4.3) is a good assumption when estimating the expected SINR for different antenna-terminal ratios.

The interference will have an impact on how many antennas the BS needs to

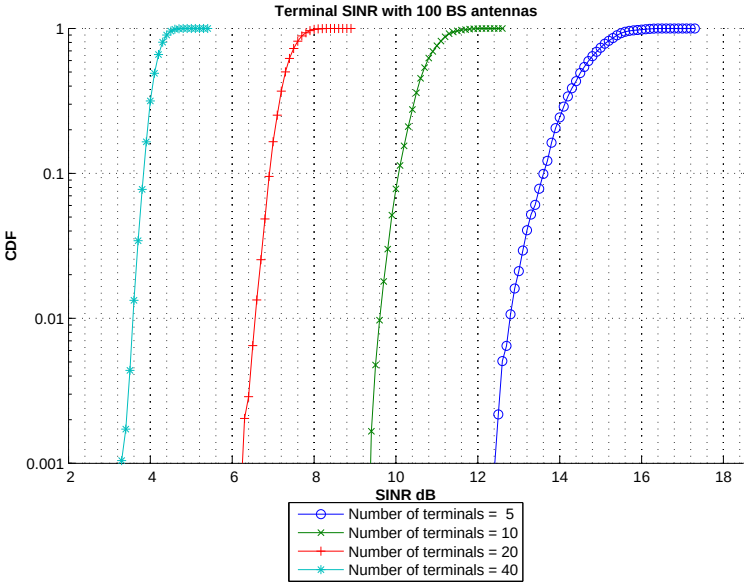

Figure 5.6: *SINR for non-moving terminals and with 100 BS antennas.*

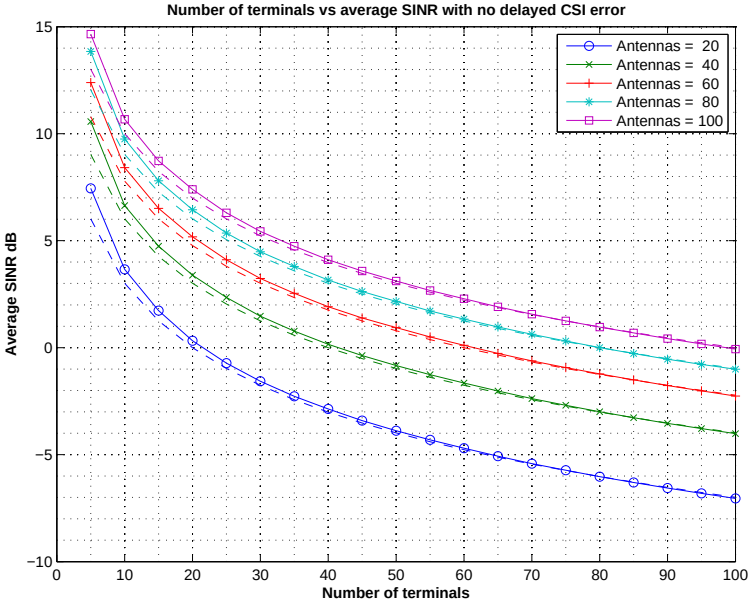

Figure 5.7: *Comparison between the simulated mean SINR and the theoretical SINR. The dashed lines represent the theoretical value from* (4.3).

be equipped with. For example, we showed in section 5.1.2 that the throughput saturated at 9 Mbps when the SINR > 20 dB. Spatial-multiplexing 2 terminals that require the highest possible throughput of 9 Mbps, they would each need an SINR $\approx$ 20 dB. Extracting M from (4.3), the BS would need approximately 200 antennas to serve 2 terminals with 9 Mbps each. More generally, spatial-multiplexing K terminals, where $K > 1$, requires approximately $100K$ BS antennas to achieve 9 Mbps for all K terminals.

5.3 Channel State Information

The problem with the delayed CSI error in section 2.3.2 is related to the coherence time. The coherence time is commonly defined as the time the channel is assumed to be constant. There is not an exact definition for the coherence time but it is normally inversely proportional to the terminal velocity, for example in [8, equation (18.20)], the rule of thumb for the coherence time T_0 is approximated as

$$T_0 \approx \frac{0.423\lambda}{V}, \tag{5.1}$$

where V is the velocity and λ is the signal wavelength.

In order to get an understanding about how fast the channel changes, we study the autocorrelation function (ACF) of the channel estimates for terminal i defined as

$$r(k) = \frac{1}{M|S|} \sum_{s \in S} \sum_{m=1}^{M} h_{i,m}^{s} \bar{h}_{i,m}^{s-k}, \tag{5.2}$$

where S is the set of channel estimates, $|S|$ is the number of channel estimates and $\bar{h}$ is the complex conjugate of the channel estimate.

The normalized ACF is appropriate when investigating small-scale fading since it removes the impact of the large-scale fading coefficient, it is defined as

$$\bar{r}(k) = \frac{r(k)}{|r(0)|}. \tag{5.3}$$

Normalized ACF values close to 1 means highly correlated channel estimates. The normalized correlation of two consecutive channel estimates is given by $\bar{r}(1)$. The channel estimates in this thesis are based on the SRS, for simplicity, the normalized correlation of two consecutive channel estimates will be referred to as the *SRS correlation*. The SRS correlation will therefore give an indication of how much the channel has changed since the last SRS transmission, low SRS correlation indicates rapid channel changes and implies higher delayed CSI error. Next section will estimate the loss in SINR depending on the SRS correlation. The normalized correlation when $k > 1$ gives an indication of how often the SRS should be transmitted. Less frequent SRS transmissions allow to serve more terminals, see Table 4.2.

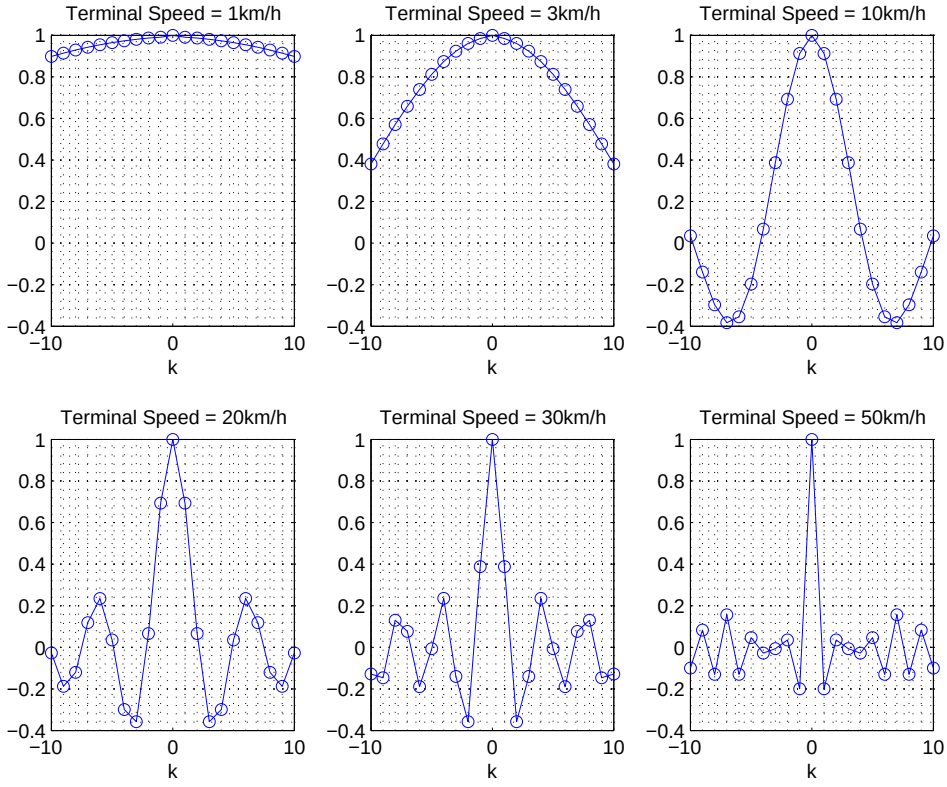

Figure 5.8: *Normalized ACF for the channel estimates where the x-axis is the correlation in steps of 5 ms for a moving terminal at different speeds.*

The normalized ACF in Figure 5.8 shows how much the channel estimates is correlated in steps of 5 ms. The figure illustrates how fast the channel changes in time and gives an indication of the coherence time. We can see that the coherence time is inversely proportional to the speed as stated in (5.1) by observing how the correlation decreases when the velocity increases.

Figure 5.8 shows that the channel estimates are highly correlated for low terminal speeds. The terminal with speed of 30 km/h should have more frequent SRS transmissions than the terminal with speed of 1 km/h, the number of SRS resources for each terminal could be dynamical scheduled by computing the ACF. The SRS correlation depend on the periodicity of the SRS transmission, SRS transmission periodicity of 5 ms will give the SRS correlation at $k = 1$ in Figure 5.8, periodicity of 10 ms will have the SRS correlation at $k = 2$ etc. By comparing the figures, the correlation when having a moving terminal at 10 km/h with an SRS periodicity of 15 ms, is approximately the same as a terminal moving at 30 km/h with an SRS periodicity of 5 ms. The result is quite obvious, the distance moved in 5 ms at 30 km/h is the same as moving at 10 km/h in 15 ms. The correlation for both

velocities is then computed in a point 4.2 cm from the starting position, remember Figure 2.3.

To get an understanding of how a moving terminal gets affected by the delayed CSI error, a simulation is performed with the terminal from section 5.1.1 with 100 BS antennas. Figure 5.9 shows how the SINR decreases when the terminal is moving at higher speeds. The SRS transmission periodicity is set to 5 ms which implies two SRS transmissions in each radioframe. The SRS correlation for the different terminal speeds can be seen for $k = 1$ in Figure 5.8. By combining Figure 5.8 and Figure 5.9, it further concludes that a low SRS correlation gives a higher SINR variance.

Note the shape of the curve for the terminal moving at 50 km/h. The simulator calculates one SINR value for every downlink subframe, the SRS periodicity of 5 ms corresponds to three consecutive downlink subframes until next SRS transmission. The shape of the curve indicates that the first downlink subframe after SRS transmission has an SINR above 32 dB, the second has SINR above 30 dB and the third has SINR below 27 dB.

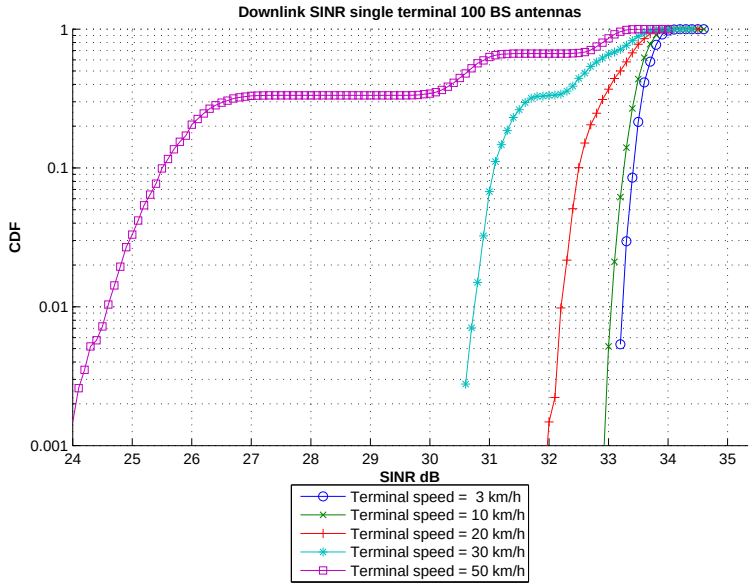

Figure 5.9: *SINR for a single moving terminal with 5 ms SRS periodicity.*

Chapter 6 will discuss how to reduce the impact of channel ageing.

5.4 Delayed CSI Error

The delayed CSI error is studied by keeping the terminal speed fixed and adjusting the frequency of the SRS transmissions. The delayed CSI error could also

be studied by keeping the SRS transmission periodicity constant and instead adjusting the terminal speed. The previous section showed that higher terminal speed gives more SINR variations and lower SRS correlation. The simulations were chosen to have moving terminals at 3 km/h and vary the SRS periodicity. The motivation to vary the SRS periodicity is because it limits the maximum number of served terminals in a cell due to the SRS resource limitation described in section 4.2. In other words, how will moving terminals be affected in terms of the delayed CSI error when increasing the SRS periodicity in order to serve more terminals?

5.4.1 Simulations

The simulated system had 100 BS antennas and 20 terminals moving at 3 km/h. Section 5.2 showed that according to our MRT precoder, the effect of large-scale fading diminishes when having interference from other terminals. The slow-scale fading depends on the terminal speed, all terminals move at 3 km/h and combined with the fact that the large-scale fading diminishes, the terminals should experience the same SINR even with the delayed CSI error.

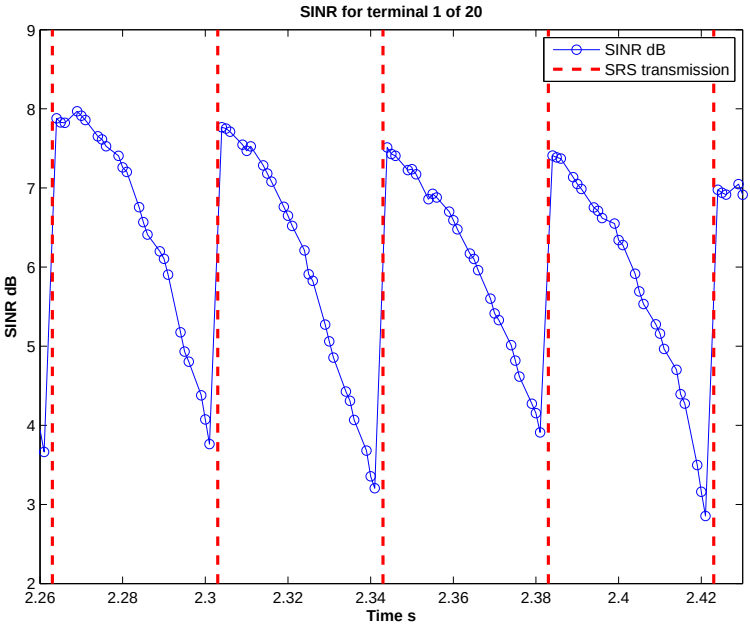

Figure 5.10: *The SINR for an arbitrary chosen terminal with SRS transmissions periodicity of 40 ms in a system with 100 BS antennas and 20 terminals.*

The SINR for an arbitrary chosen terminal is shown in Figure 5.10, the figure illustrates how the SINR decreases with the time difference to the latest SRS transmission. The figure illustrates how precoding with old CSI affects the SINR during a short time interval, the shape of the curve indicates that the decrease

in SINR is not linear in time and the variation in SINR will increase rapidly with less frequent SRS transmissions.

The SINR for the 20 terminals is shown in Figure 5.11, the figure illustrates how the SINR in the 10th, 50th and 90th percentile decreases with less frequent SRS transmissions. We observe by study the difference between the 10th and the 90th SINR percentile that the variation in SINR increases with less frequent SRS transmissions. For example, the difference between the 10th and 90th SINR percentile is approximately 1 dB with SRS periodicity of 20 ms and approximately 17 dB with SRS periodicity of 80 ms. The SINR in the 10th percentile is of particular interest since the link adaptation discussed in section 4.6 adapts the MCS based on the 10th SINR percentile, this means that the terminal throughput will be limited by the 10th SINR percentile.

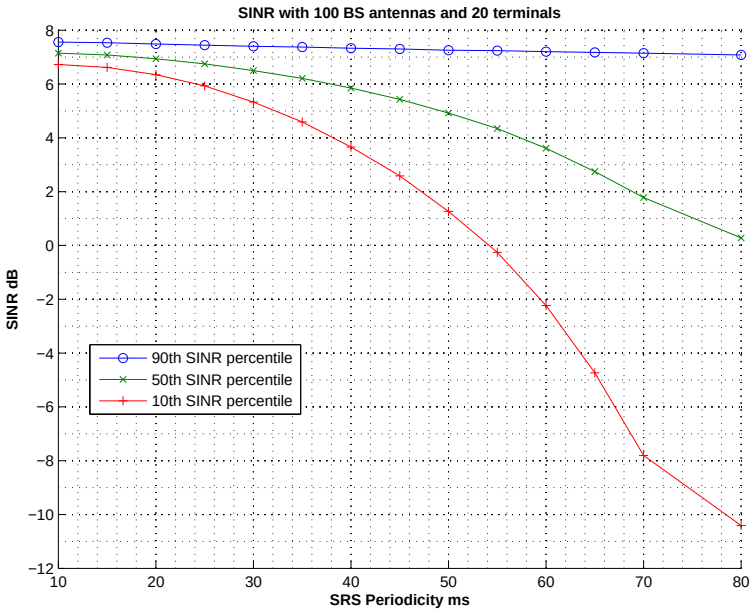

Figure 5.11: *SINR for 20 terminals with different SRS periodicities and 100 BS antennas.*

The SRS periodicity affects the SINR, previous section showed that longer SRS periodicity gave a lower SRS correlation, it is therefore interesting to see the loss in SINR compared to non-moving terminals. Non-moving terminals has an SRS correlation close to 1. The loss in the 10th SINR percentile is illustrated in Figure 5.12, the figure shows a simulation of 20 terminals when iterating over different SRS transmission periodicities and therefore, different SRS correlations. The dashed line is a second-degree polynomial approximation between the SRS correlation and the loss in the 10th SINR percentile. For example, when considering a moving terminal at 10 km/h with an SRS periodicity of 15 ms. The

SRS correlation of 0.38 is obtained from Figure 5.8, plugging in the SRS correlation in the second-degree polynomial approximation gives an approximate 6 dB loss in the 10th SINR percentile. The result in terms of SINR loss could be applied to other antenna-terminal ratios since the variations in SINR caused by the delayed CSI error depends on the propagation environment and not by the antenna-terminal ratio.

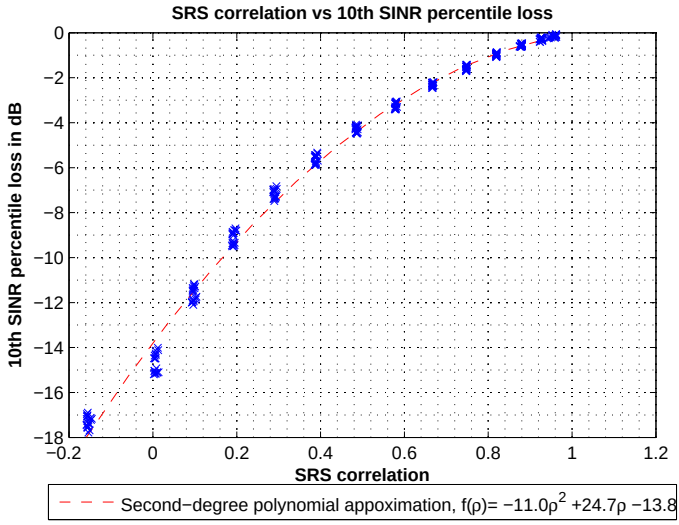

Figure 5.12: *SRS correlation vs 10th SINR percentile loss. The loss in the 10th SINR percentile caused by the delayed CSI error.*

5.4.2 Discussion

The simulations show that more frequent SRS transmission can reduce the delayed CSI error. The downside of more frequent SRS transmission is a decrease in the maximum number of served terminals since the resources for SRS are limited.

5.5 Link Adaptation

The link adaptation sets the MCS, the MCS determines how many data bits that is transmitted in each transport block. The link adaptation will therefore affect the throughput result in this thesis, this section discusses the thesis chosen link adaptation.

The link adaptation in this thesis adapts the MCS to a block error rate target of 10%. Use of higher MCS can increase the data rate if the transmission is successful. Since we use a block error rate target of 10%, the MCS will be based on the 10th

SINR percentile. Figure 5.11 in the previous section with an SRS periodicity of 80 ms corresponds to an MCS based on an SINR ≈ -10 dB.

We will compare the chosen block error rate target with a block error rate target of 50% to illustrate that the chosen link adaptation is not optimal in all situations. If the link adaptation instead is targeted to a block error rate target of 50%, the MCS will be based on the 50th SINR percentile. This means for an SRS periodicity of 80 ms in Figure 5.11, that it might be better to succeed with 50% of the transmissions with an MCS based on an SINR ≈ 0 dB, compared to succeeding with 90% of the transmissions with an SINR ≈ -10 dB.

The terminal throughput is simulated when the BS has a block error rate target of 10%, respectively 50%. The BS has 100 antennas and serves 20 moving terminals at 3 km/h. Figure 5.13 and Figure 5.14 shows the terminal throughput with a block error rate target of 10%, respectively 50%. By comparing the figures, we observe an increased throughput with a block error rate target of 50% compared with a block error rate target of 10% for an SRS periodicity of 60 ms and 80 ms. The mean terminal throughput for an SRS periodicity of 80 ms is 0.4 Mbps with a block error rate target of 10% and 1.3 Mbps with a block error rate target of 50%.

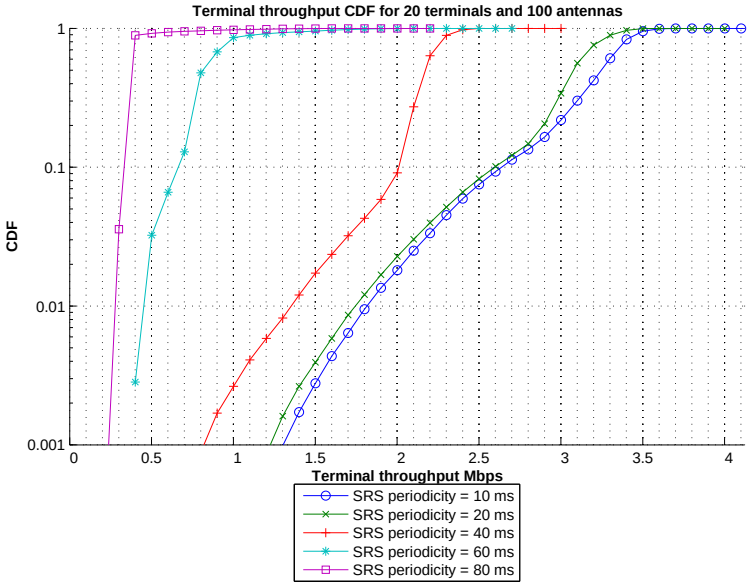

Figure 5.13: *Terminal throughput CDF for 20 moving terminals at 3 km/h when BS has a block error rate target of 10%.*

The figures in this section illustrate the importance of proper link adaptation. Sometimes, it is better in terms of terminal throughput to have another block error rate target than 10%. The cell throughput simulations in the next sections will have moving terminals at 3 km/h and an SRS periodicity of 20 ms. We observe in Figure 5.13 and Figure 5.14 that link adaptation based on a block error rate

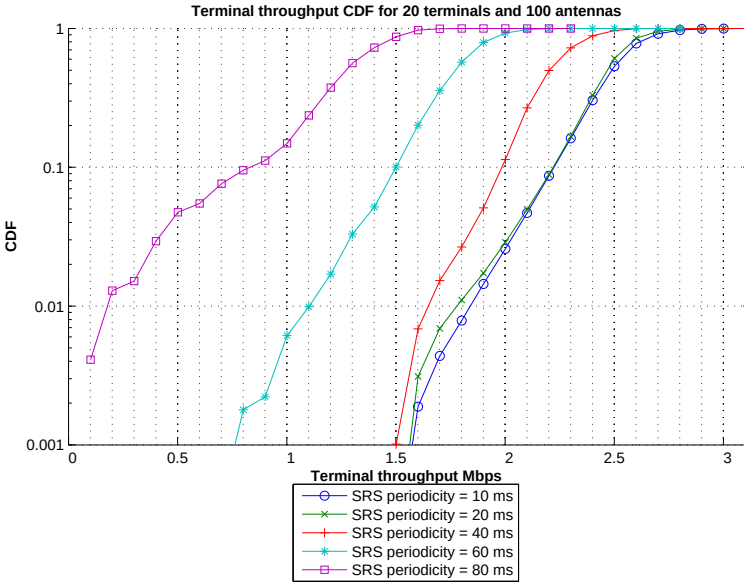

Figure 5.14: *Terminal throughput CDF for 20 moving terminals at 3 km/h when BS has a block error rate target of 50%.*

target of 10% performed better than a block error rate target of 50% in this case. The thesis did not investigate other block error rate targets and we will therefore select a block error rate target of 10% in subsequent sections.

Note that the curve characteristics in Figure 5.10 could be used in order to have a link adaptation that takes the time difference to the last SRS transmission into account when setting the MCS. The figure shows how the SINR decreases after the SRS transmission, the link adaptation could then set a higher MCS just after the SRS transmission and a lower MCS just before the next SRS transmission.

5.6 Cell Throughput

The cell throughput simulations have full buffer terminals moving at 3 km/h with an SRS periodicity of 20 ms.

Figure 5.15 illustrates how the cell throughput increases when the number of spatial-multiplexed terminals increases. Compare the figures with no spatial-multiplexed terminals in section 5.1.2 where the maximum cell throughput is 9.0 Mbps. Figure 5.15 shows that the cell throughput with 90% probability is above 40 Mbps with 10 terminals. The difference between the 10th and 90th cell throughput percentile is less than 6 Mbps for all four terminal configurations. We also observe that the increase in mean cell throughput is approximate 20 Mbps when increasing from 10 to 20 terminals. The SINR for the terminals is showed in

Figure 5.16, by utilizing the fact that link adapatation is based on the 10th SINR percentile, we can state that it is better in terms of cell throughput to have 20 terminals with 6.4 dB in the 10th SINR percentile than 10 terminals with 9.6 dB in the 10th SINR percentile. The increase in cell throughput is 20 Mbps.

The terminal throughput decreases for the 20 terminal case compared to the 10 terminal case. The reduced terminal throughput is due to the fact that the interference increases. The terminal throughput is calculated by dividing the cell throughput with the number of terminals, the mean terminal throughput is 4.0 Mbps respectively 3.0 Mbps for the 10 and 20 terminal case. Compare this with a maximum cell throughput of 9 Mbps when scheduling the terminals into separate time-frequency resources, this gives a maximum terminal throughput of 0.9 Mbps respectively 0.45 Mbps for the 10 and 20 terminal case.

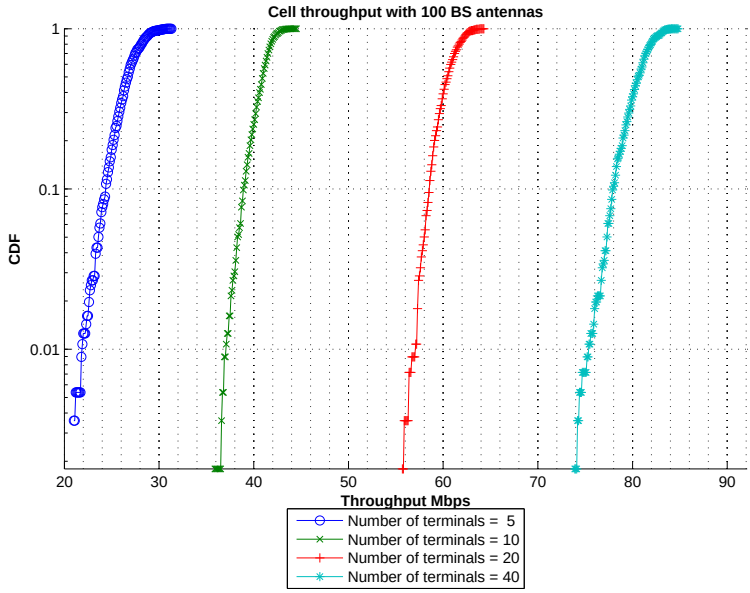

Figure 5.15: *Cell throughput with moving terminals at 3 km/h and an SRS transmission periodicity of 20 ms.*

Figure 5.15 illustrates the variation in cell throughput. We can for example see for the 20 terminal case, the mean cell throughput is 60 Mbps, and the cell throughput is above 56.5 Mbps with 99% probability. The low variation in cell throughput should be kept in mind for the next section that will only study the average cell throughput for different antenna-terminal configurations.

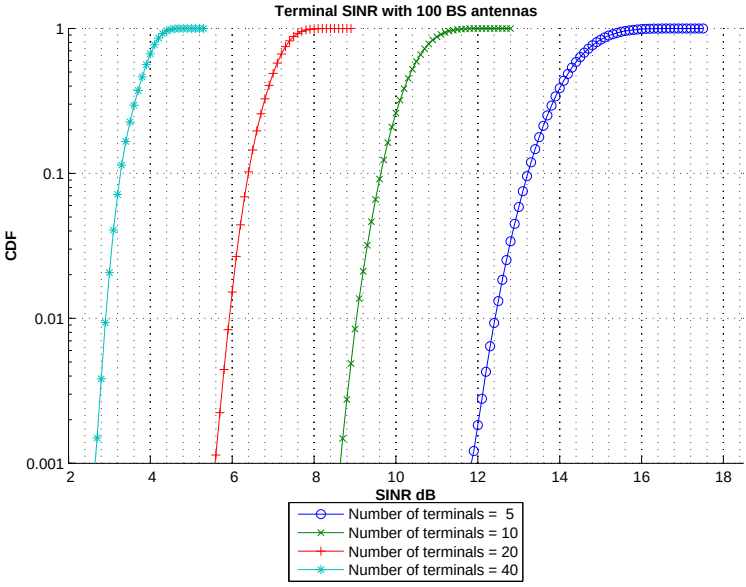

Figure 5.16: *Terminal SINR with moving terminals at 3 km/h and an SRS transmission periodicity of 20 ms.*

5.7 Maximization of Average Cell Throughput

The cell throughput is studied for more antenna-terminal configurations in order to determine the ratio between the number of BS antennas and the number of terminals that maximizes the average cell throughput. The previous section showed low variations in cell throughput, the mean cell throughput is therefore close to the maximum value. The SINR results from section 5.2 showed that the expected SINR is close to the theoretical result in (4.3). The resulting cell throughput when increasing the number of terminals should therefore have the same curve characteristics as in Figure 2.4.

The simulation is performed by studying non-moving terminals, which will not suffer from the delayed CSI error, and moving terminals at 3 km/h. The non-moving terminal simulation will only suffer from interference. When having no delayed CSI, the result is not affected by the SRS transmission periodicity, which allows more terminals to be scheduled. Figure 5.17 shows how the mean cell throughput increases when the number of terminals increases. The figure illustrates the optimization problem of how many terminals that should be spatial-multiplexed when maximizing the cell throughput. Since the maximum degrees of freedom is $\min(M, K)$, we only consider scenarios when the number of terminals is less than the number of BS antennas. We observe in the figure that the number of BS antennas equal to the number of terminals is a reasonable assumption when maximizing the cell throughput, i.e., $\alpha \approx 1$.

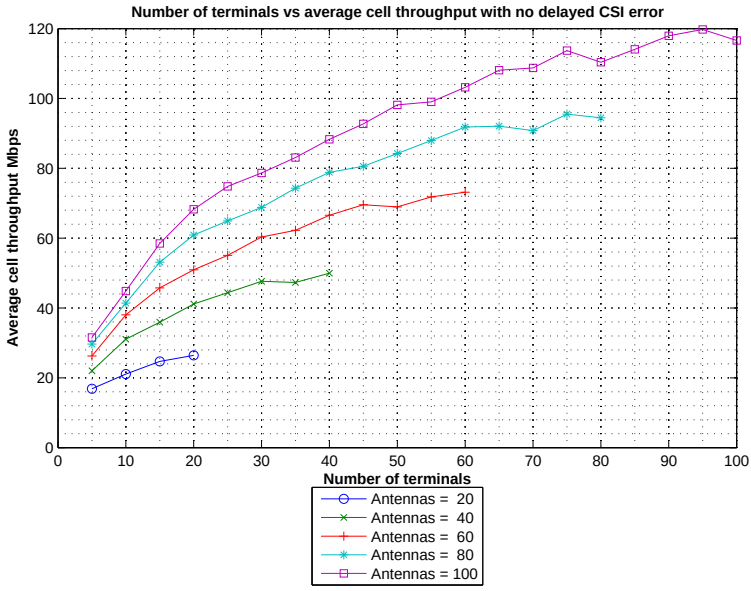

Figure 5.17: *Average cell throughput with no delayed CSI error and with various number of BS antennas.*

A simulation with moving terminals at 3 km/h and an SRS periodicity of 20 ms is displayed in Figure 5.18 for comparison. The maximum number of served terminals is 96 according to Table 4.2. Note that the curve with 100 BS antennas is not plotted with 100 terminals due to this limitation, however, the curve characteristics shows that the throughput had not been increased significantly with 100 terminals. The figure also concludes that putting the number of BS antennas equal to the number of terminals is a reasonable assumption when maximizing the cell throughput. The maximum cell throughput in Figure 5.18 is 106 Mbps for the 100 BS antennas case compared to 120 Mbps in Figure 5.17, the decreased cell throughput of approximately 13% is because of using old CSI.

The maximum average cell throughput with no delayed CSI error is related to the number of BS antennas in Figure 5.19. The figure gives an indication of how many antennas the BS should be equipped with to meet cell throughput demands. The linear approximation can be used to estimate the required number of antennas for a given cell throughput demand. Note that this thesis operated in the interference limited regime and used the MRT precoder defined in (4.1).

If we instead want to calculate the required number of BS antennas to meet a terminal throughput demand for moving terminals, we can combine the result from previous sections to estimate the number of BS antennas, one example is illustrated in the appendix.

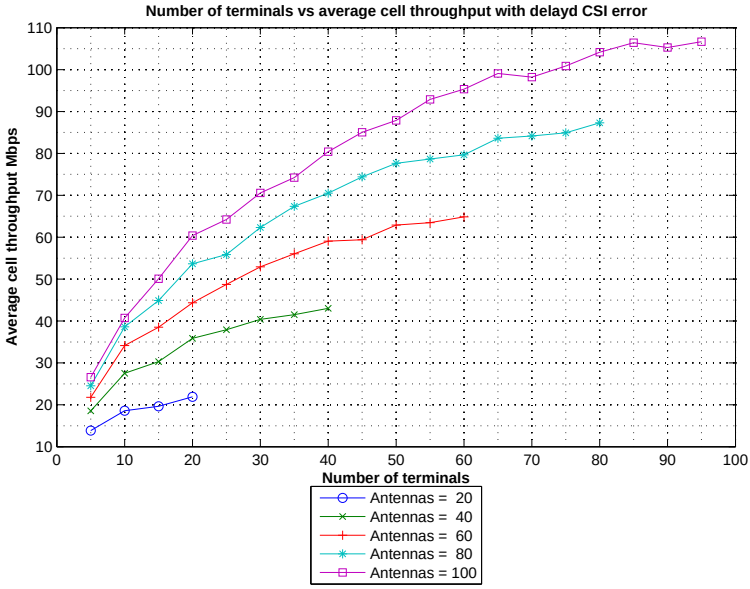

Figure 5.18: *Average cell throughput with moving terminals at 3 km/h and an SRS transmission periodicity of 20 ms with various number of BS antennas.*

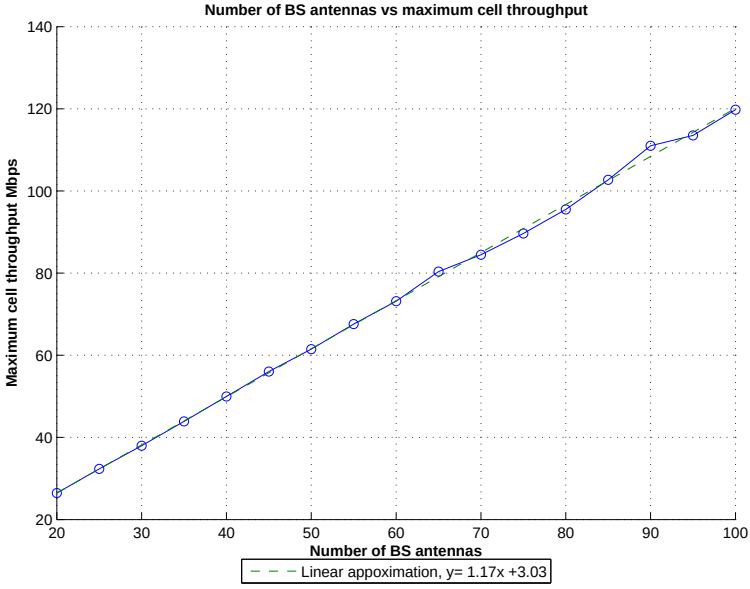

Figure 5.19: *Number of BS antennas vs maximum average cell throughput when having no delayed CSI error.*

6 Discussion

This chapter discusses point 3 in the problem statement, "How does the chosen LTE configuration in Chapter 4 affect the CSI acquisition and the maximum terminal throughput?". We also give some suggestions of how the throughput could be increased and how to reduce the delayed CSI error.

6.1 CSI Acquisition

The BS calculates CSI from the SRS. In this study, the maximum number of terminals served in a cell depends on the SRS transmission frequency and the number of uplink subframes.

The TDD configuration had 4 OFDM symbols allocated for SRS in each radioframe and 12 terminals could transmit SRS during one OFDM symbol. Introducing more resources for SRS could be used to serve more terminals. More SRS resources could also be used for more frequent channel acquisition at the BS which would reduce the effect of channel ageing. For example, the simulations showed that two consecutive channel estimates are nearly uncorrelated for a moving terminal at 50 km/h with SRS periodicity of 5 ms. More frequent SRS transmission cannot be achieved in our TDD configuration which imposes that the amount of SRS resources will probably not be sufficient when considering a moving terminal at 300 km/h.

The simulations assumed full buffer, the data traffic in full buffer can be seen as downloading a huge file or streaming video. Terminals with web traffic receive data during short time periods. The SRS transmissions could be limited to transmit when the terminal has a pending data reception and thus, more available SRS resources for full buffer terminals.

The simulations were performed with all terminals having the same SRS transmission frequency, the terminals were also moving at the same speed. In practice, the terminals have different speeds and the SRS transmission frequency affects the reception quality of the terminals differently. An improved scheduler could vary the frequency of the SRS transmissions for each terminal by estimating the delayed CSI error. This thesis estimated the delayed CSI error by calculating the normalized correlation of two consecutive channel estimates. The scheduling could also take the time difference into account from the terminals last SRS transmission and schedule terminals closer in time to their SRS transmission, and reduce the impact of the delayed CSI error.

6.2 Throughput

This section discusses how the terminal throughput could be increased by allocating more resources for downlink transmission and support other modulations.

6.2.1 MCS

The simulations showed that the terminal throughput saturated at 9.0 Mbps when the SINR is approximately 20 dB. The BS is then transmitting with the highest possible MCS. With no spatial-multiplexed terminals in a system with 100 BS antennas, the SINR is above 45 dB for approximately 90% of the terminals. If using higher modulation such as 128QAM, the throughput could be increased for terminals with high SINR.

6.2.2 Resource Allocation

The terminal throughput result is affected by the chosen fraction of resources allocated for PDSCH, the PDSCH occupied 42% of the resources in the time-frequency grid. Another resource allocation would have resulted in another outcome. The bandwidth used was 5 MHz, scaling up to 10 MHz or 20 MHz bandwidth would scale the results with a factor of 2 respectively 4. For example, 20 MHz bandwidth would increase the maximum terminal throughput to 36 Mbps, remember Figure 5.3.

In this thesis, the scheduling limitations was not taken into account, the PDCCH has a limited amount of resources and can not schedule an unlimited amount of terminals. The PDCCH was assigned to the first 3 OFDM symbols in each downlink subframe in order to include resource allocation for control signalling. In Massive MIMO, the resource allocation for control signalling could be reduced by beamforming the terminal specific control data in the same time-frequency resource. The PDCCH will then mainly contain broadcast data and occupy less time-frequency resources. The *Enhanced PDCCH* in LTE release 11 was implemented with the main goal to achieve spatial reuse of the control channel resources [10]. Having less resource assignments for control signalling, we could allocate more resources for the PDSCH and increase the throughput.

7

Conclusions

This thesis investigated Massive MIMO with an MRT precoder in a single-cell deployment. The important assumptions and simulator parameters for this thesis is presented in Table 4.1.

The problem formulation had five different investigations that will be considered individually below.

1. *How do spatial-multiplexing terminals into the same time-frequency resource affect the expected SINR and the throughput?*

    - The result from (4.3) states that the expected SINR depends on the ratio between the number of BS antennas and the number of terminals. With perfect CSI at the BS, the simulated SINR for different antenna-terminal ratios was close to the value in (4.3), which means that the expected SINR with a fixed number of BS antennas is limited by the interference from other terminals.

      For example, with 100 BS antennas and non-moving terminals, 10 terminals had a mean SINR of 10.5 dB, increasing to 20 terminals resulted in a mean SINR of 7.5 dB. The 3 dB loss for doubling the number of terminals or halving the number of BS antennas was also seen for other antenna-terminal ratios.

    - The terminal throughput decreases when increasing the number of spatial-multiplexed terminals.

      For example, with 100 BS antennas and moving terminals at 3 km/h with an SRS transmission periodicity of 20 ms. The mean terminal throughput is 4.0 Mbps when spatial-multiplexing 10 terminals and

3.0 Mbps with 20 spatial-multiplexed terminals.

- The simulations showed that the cell throughput increased with more spatial-multiplexed terminals. The thesis compared the results with no spatial-multiplexed terminals which gave a maximum cell throughput of 9 Mbps. With spatial-multiplexed terminals, 120 Mbps cell throughput could be achieved with 100 BS antennas when having non-moving terminals. In other words, with 100 BS antennas, the maximum cell throughput increased approximately 13 times with spatial-multiplexed terminals compared with no spatial-multiplexed terminals.
- The maximum cell throughput decreased with 13% for a BS with 100 antennas when having moving terminals at 3 km/h with an SRS transmission periodicity of 20 ms compared to a system with non-moving terminals.

2. *How does channel ageing affect SINR?*
   - The variation in SINR increased rapidly with less frequent SRS transmissions.

     For example, when having moving terminals at 3 km/h, the difference between the 10th and 90th SINR percentile is approximately 1 dB with an SRS periodicity of 20 ms and approximately 17 dB with an SRS periodicity of 80 ms.
   - The normalized correlation of two consecutive channel estimates was used to derive a second order polynomial approximation of the 10th SINR percentile loss. For example, a moving terminal at 10 km/h with SRS transmission periodicity of 15 ms had a 6 dB loss in the 10th SINR percentile compared to non-moving terminals.
3. *How does the chosen LTE configuration in Chapter 4 affect the CSI acquisition and the maximum terminal throughput?*
   - The TDD configuration had 4 OFDM symbols allocated for SRS in each radioframe and 12 terminals could transmit SRS during one OFDM symbol. Introducing more resources for SRS would thus allow to serve more terminals. More SRS resources could also be used for more frequent channel acquisition at the BS which could reduce the effect of the delayed CSI error.
   - The terminal throughput saturated at 9.0 Mbps when the terminal SINR is approximately 20 dB.
4. *What is the ratio between the number of BS antennas and the number of terminals that maximizes the cell throughput?*
   - The simulation showed that the number of BS antennas equal to the number of spatial-multiplexed terminals is a reasonable ratio when

maximizing the cell throughput.

- The maximum cell throughput scaled linearly with the number of BS antennas.

5. *What is the required number of BS antennas in order to maximize the terminal throughput?*

   - The terminal throughput saturated at 9.0 Mbps when the terminal SINR is approximately 20 dB. Serving K non-moving terminals, where $K > 1$, and each terminal require the highest throughput of 9 Mbps, the BS should be equipped with approximately $100K$ antennas.

8

Further Research

This thesis investigated Massive MIMO in LTE, the thesis was an overall investigation and the problems encountered need to be studied more in depth. The recommended further research in this chapter is based on the encountered problems and the assumptions made in this thesis. The thesis suggested further research is given below.

- Multiple cells - the only interference considered was intra-cell interference. If studying multiple cells, investigation of inter-cell interference and *pilot contamination* are needed. Pilot contamination is when the channel estimates in the cell is contaminated by pilots from other cells [15].
- Channel ageing - the thesis showed how precoding with old CSI affected the SINR. To reduce the problems with channel ageing, further investigations in link adaptation and uplink pilot transmission are needed. Channel predictions suggested by [19] could reduce the problems with channel ageing. The idea behind channel prediction is to use current and past channel observations to predict future channel realizations.
- Precoder - the thesis used an MRT precoder according to (4.1). The MRT precoder in (2.9), or a *zero-forcing precoder* could improve the results and should thus be investigated. The zero-forcing precoder has the property to null out the interference from other terminals and the performance with fixed number of antennas is mainly limited by the transmitter power [17]. The drawback of zero forcing is that it contains a computational heavy matrix inverse.
- Reciprocal channel - the CSI was obtained by assuming a reciprocal channel. The reciprocal channel assumption needs to be further investigated. Addi-

tionally, the hardware needs to be calibrated in order to assume a reciprocal channel, see [18].

- MCS in LTE - the terminal throughput saturated at 9 Mbps for our LTE configuration. The increase in SINR with more BS antennas could be used to increase the terminal throughput and should thus be investigated, for example, support modulation with 128QAM.
- Uplink - the thesis only considered downlink transmission, uplink should be investigated since it can also take advantage of more BS antennas [15].

In short, Massive MIMO has big potential but there are still many unresolved issues to tackle before a commercial deployment.

Appendix

A

Terminal Throughput Demand

The result from Chapter 5 is combined to estimate how many antennas the BS needs to be equipped with to meet a throughput demand for K moving terminals.

Figure A.1 illustrates the work flow to calculate the number of antennas. This derivation should be seen as a rule of thumb for how many antennas the BS need and Chapter 4 should be taken into account when studying the results below. The derivation for the number of BS antennas is illustrated in example A.1.

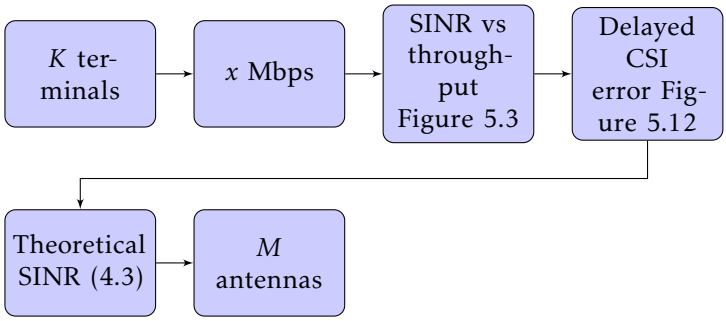

Figure A.1: *Block diagram for estimating the number of required BS antennas for a given number of K terminals with a throughput requirement.*

A.1 Example

We want to derive the number of BS antennas for 20 moving terminals at 3 km/h that have an SRS transmission periodicity of 20 ms. The required terminal throughput is 3 Mbps, which implies a cell throughput of 60 Mbps.

We start by extracting the SINR from Figure 5.3. With 3 Mbps required throughput, the terminals need SINR ≈ 7.66 dB.

The SRS correlation for a moving terminal is extracted from the second plot in Figure 5.8, each circle corresponds to the SRS correlation in steps of 5 ms so the resulting SRS correlation is located at $k = 4$ and is 0.874.

The 10th percentile SINR loss due to the SRS correlation is calculated by using the second degree polynomial from Figure 5.12. The loss in SINR due to the delayed CSI error is

$$f(0.874) = -11.005 \cdot (0.874^2) + 24.7225 \cdot 0.874 - 13.7291 = 0.58 \text{ dB}.$$

The required SINR y is

$$y = 7.66 + 0.58 = 8.24 \text{ dB}.$$

Rewriting (4.3) when using logarithmic SINR values gives

$$\alpha = 10^{(y/10)}$$

$$\alpha = \frac{M}{K} \Rightarrow //K = 20// \Rightarrow$$
$$\Rightarrow M = 20\alpha = 134.$$

The result is evaluated by simulating the terminal throughput for the 20 terminals. Figure A.2 shows the evaluation for the 3 Mbps throughput demand but also when the terminal throughput target is 1 Mbps and 2 Mbps. The terminal throughput target of 1 Mbps and 2 Mbps were derived with the same procedure and gave 24 respectively 66 BS antennas. The figure shows that the quality of reception goal is fulfilled for 99.5% of the terminals for the three different terminal throughput goals.

Figure A.3 gives an indication of how many antennas the BS should be equipped with in order to serve 20 terminals with a required quality of service. The figure illustrates how the number of required BS antennas increases rapidly when the SRS correlation decreases. Note that this was performed with a link adaptation based on a block error rate target of 10%. We have seen that another block error rate target can in some cases perform better in terms throughput, and thus, the result could be improved in terms of less BS antennas.

The Matlab code for deriving the number of antennas is given below.

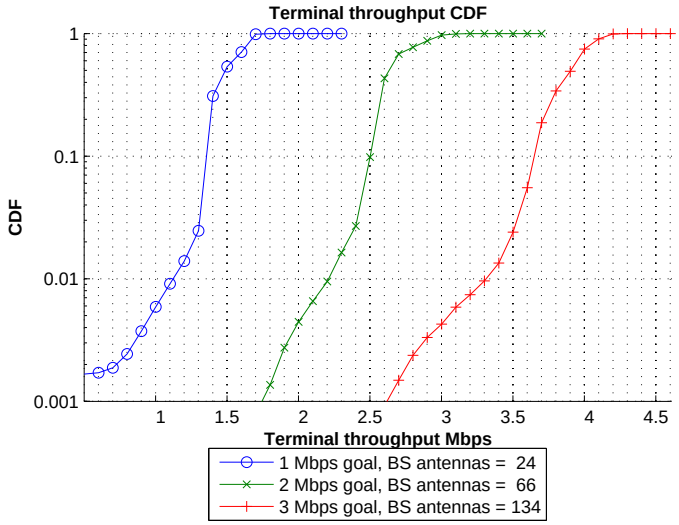

Figure A.2: *Evaluation of the terminal throughput demand for the 20 terminals in example A.1.*

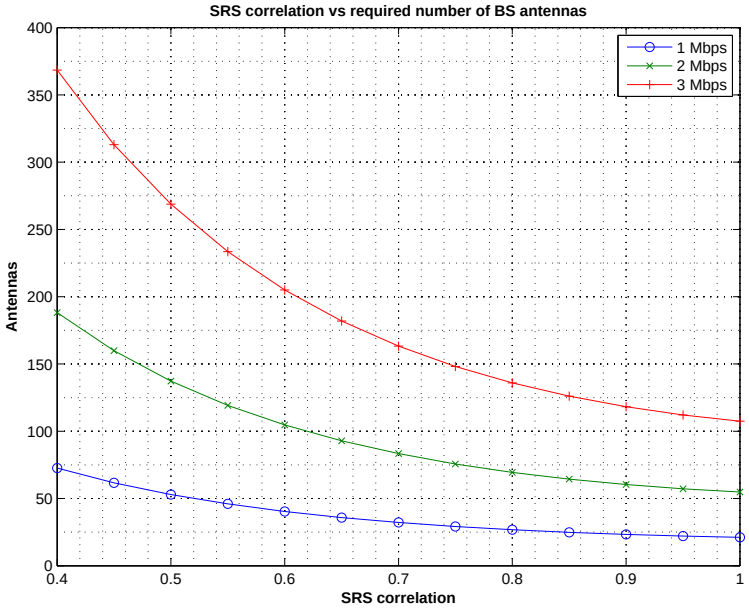

Figure A.3: *SRS correlation vs required number of BS antennas when having 20 terminals with a required quality of service.*

Matlab Code

```
%function that calculates the number of BS antennas given
%K terminals,SRS correlation and throughput demand
function M = calculateRequiredNumAntennas(K,correlation,Mbps)
dBlossPolynom = [-10.0028   23.3695  -13.3698]; %delayed CSI
throughput=[ 0.003274 0.044410 0.084119 0.091338 0.115516 ...
    0.135916 0.136252 0.142716 0.191995 0.272588 0.384677 ...
    0.458529 0.546500 0.679390 0.826254 1.007422 1.207288 ...
    1.453291 1.707046 1.916168 2.195320 2.524613 2.863536 ...
    3.237570 3.591611 3.885764 4.256202 4.621004 5.154913 ...
    5.593996 6.052807 6.650850 7.212053 8.076326 9.025067 ...
    9.035947 9.035947 9.035947 9.035947 9.035947 9.035947 ...
    9.035947 9.035947 9.035947 9.035947 9.035947 9.035947 ...
    9.035947 9.035947 ];
sinr=[-14.660364 -13.691264 -12.722164 -11.650064 -10.680964 ...
       -9.711864  -8.708159  -7.725293  -6.701564  -5.697859 ...
       -4.714998  -3.691279  -2.704834  -1.704718  -0.702681 ...
        0.296741   1.298651   2.296406   3.298237   4.298404 ...
        5.298560   6.297637   7.298342   8.297878   9.298165 ...
       10.298244  11.298718 12.298274  13.298473  14.298387
...
       15.298420  16.298353 17.298302  18.298330  19.298461
...
       20.298473  21.298467 22.298459  23.298449  24.298465
...
       25.298440  26.298444 27.298455  28.298452  29.298447
...
       30.298447 31.298447 32.298448 33.298449];
reqSINR = interp1(throughput(1:36),sinr(1:36), Mbps);
dbLossReciprocity = correlation^2*dBlossPolynom(1) ...
    +correlation*dBlossPolynom(2)+dBlossPolynom(3);
reqSINR = reqSINR-dbLossReciprocity;
alfa = 10^(reqSINR/10);
M = alfa*K;
M = round(M);
```

Bibliography

[1] Rec. ITU-R M.1225 1. *Guidelines for evaluation of radio transmission technologies for IMT-2000*. 1997. Cited on page 9.

[2] 3GPP 25.814. *3rd Generation Partnership Project; Technical Specification Group Radio Access Network; Physical layer aspects for evolved Universal Terrestrial Radio Access (UTRA) (Release 7)*. 2006. URL `http://www.qtc.jp/3GPP/Specs/25814-710.pdf`. Cited on pages 17 and 23.

[3] 3GPP 36.211. *Evolved Universal Terrestrial Radio Access (E-UTRA); Physical channels and modulation*. 2006. URL `http://www.3gpp.org/DynaReport/36211.htm`. Cited on page 15.

[4] 3GPP 36.212. *Evolved Universal Terrestrial Radio Access (E-UTRA); Multiplexing and channel coding*. 2008. URL `http://www.3gpp.org/DynaReport/36212.htm`. Cited on page 15.

[5] 3GPP 36.213. *Evolved Universal Terrestrial Radio Access (E-UTRA); PPhysical layer procedures*. 2006. URL `http://www.3gpp.org/DynaReport/36213.htm`. Cited on page 27.

[6] Ericsson AB. *Ericsson Mobility Report. November 2012*. URL `http://www.ericsson.com/res/docs/2012/ericsson-mobility-report-november-2012.pdf`. Cited on page 19.

[7] Erik Dahlman. *LTE/ LTE-Advanced for Mobile Broadband*. Elseiver Ltd, 2011. Cited on pages 12, 14, and 20.

[8] Jerry D. Gibson. *The mobile communications handbook. CRC*. Press, Inc. Boca Raton, FL, USA, 1998. Cited on page 32.

[9] Jakob Hoydis. *Channel Measurements for Large Antenna Arrays*. IEEE International Symposium on Wireless Communication Systems (ISWCS), Paris, France, August, 2012. Cited on page 22.

[10] Sravanthi Kanchi. *Overview Of LTE-A Technology*. International journal of

scientific & technology research volume 2, issue 11, november 2013, 2006. Cited on page 46.

[11] Erik G. Larsson. *Massive MIMO for Next Generation Wireless System*. IEEE Communications Magazine, Vol. 52, No. 2, pp. 186-195, Feb. 2014, 2014. Cited on page 3.

[12] T.K.Y. Lo. *Maximum ratio transmission*. IEEE Trans. on Communications, 1999. Cited on page 2.

[13] Upamanyu Madhow. *Fundamentals of Digital Communication*. Cambridge University Press, 2008. Cited on page 15.

[14] Thomas L Marzetta. *How Much Training is Required For Multiuser MIMO*. Signals, Systems and Computers, 2006. ACSSC '06. Fortieth Asilomar Conference, 2006. Cited on page 4.

[15] Thomas L Marzetta. *Noncooperative Cellular Wireless with Unlimited Numbers of Base Station Antennas*. IEEE Trans. Wireless Communications, 2010. Cited on pages 3, 51, and 52.

[16] Hien Quoc Ngo. *Massive MU-MIMO Downlink TDD Systems with Linear Precoding and Downlink Pilots*. Allerton Conference on Communication, Control, and Computing, Urbana-Champaign, Illinois, October, 2013. Cited on page 14.

[17] Fredrik Rusek. *Scaling up MIMO: Opportunities and Challenges with Very Large Arrays*. Prentice Hall, Inc., third edition, 2002. Cited on pages 4, 6, 22, and 51.

[18] Clayton Shepard. *Practical Many-Antenna Base Stations*. ACM Int Conf. Mobile Computing and Networking (MobiCom), Istanbul, Turkey, 2012. Cited on page 52.

[19] Kien T. Truong and Robert W. Heath Jr. *Effects of Channel Aging in Massive MIMO Systems*. Journal of Communications and Networks, VOL 15, NO. 4, 2013. Cited on page 51.

[20] David Tse and Pramod Viswanath. *Fundamentals of Wireless Communication*. Cambridge University Press, 2008. Cited on pages 8, 22, and 25.